Science of the Total Environment 894 (2023) 164995

Contents lists available at ScienceDirect

Science of the Total Environment

journal homepage: www.elsevier.com/locate/scitotenv

Identifying driving hydrogeomorphic factors of coastal wetland downgrading using random forest classification models

Keqi He [a], Wenhong Li [a,*], Yu Zhang [b], Ge Sun [c], Steve G. McNulty [c], Neal E. Flanagan [d], Curtis J. Richardson [d]

[a] Earth and Climate Sciences, Nicholas School of the Environment, Duke University, Durham, NC 27708, USA
[b] Earth and Environmental Sciences Division, Los Alamos National Laboratory, Los Alamos, NM 87545, USA
[c] Eastern Forest Environmental Threat Assessment Center, USDA Forest Service Southern Research Station, USDA Forest Service, Research Triangle Park, Raleigh, NC 27709, USA
[d] Duke University Wetland Center, Nicholas School of the Environment, Duke University, Durham, NC 27708, USA

HIGHLIGHTS

- Wetland downgrading was accurately (> 97 %) classified.
- Dominant hydrological mechanisms varied for different types of wetland downgrading.
- Woody wetlands were most susceptible to saltwater intrusion.
- Emergent herbaceous wetlands were most vulnerable to inundation and drought.
- Distances to canals were key to determining the fates of downgraded woody wetlands.

GRAPHICAL ABSTRACT

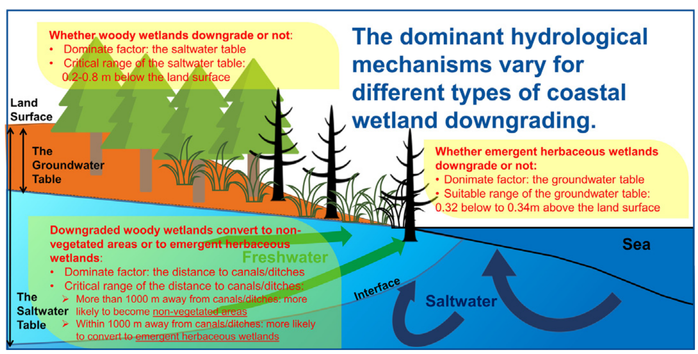

ARTICLE INFO

Editor: Jan Vymazal

Keywords:
Coastal wetland downgrading
Machine learning models
Hydrogeomorphic factors
Climate change
Sea-level rise
Anthropogenic activities

ABSTRACT

Coastal wetlands provide critical ecosystem services but are experiencing disruptions caused by inundation and saltwater intrusion under intensified climate change, sea-level rise, and anthropogenic activities. Recent studies have shown that these disturbances downgraded coastal wetlands mainly through affecting their hydrological processes. However, research on what is the most critical driver for wetland downgrading and how it affects coastal wetlands is still in its infancy. This study examined drivers of three types of wetland downgrading, including woody wetland loss, emergent herbaceous wetland loss, and woody wetlands converting to emergent herbaceous wetlands. By using random forest classification models for the wetland ecosystems in the Alligator River National Wildlife Refuge, North Carolina, USA, during 1995–2019, we determined the relative importance of different hydrogeomorphic processes and the dominant variables in driving the wetland downgrading. Results showed that random forest classification models were accurate (> 97 % overall accuracy) in classifying wetland downgrading. Multiple hydrogeomorphic variables collectively contributed to the coastal wetland downgrading. However, the dominant control factors varied across different types of wetland downgrading. Woody wetlands were most susceptible to saltwater intrusion and were likely to downgrade if the saltwater table was shallower than 0.2 m below the land surface. In contrast, emergent herbaceous wetlands were most vulnerable to inundation and drought. The favorable groundwater table for emergent herbaceous wetlands was between 0.34 m above the land surface and 0.32 m below the land surface, beyond which the emergent herbaceous wetland tended to disappear. For downgraded woody wetlands, their distance to canals/ditches played a crucial role in determining their fates after downgrading. The machine learning approach employed in this study provided critical knowledge about the thresholds of hydrogeomorphic variables for the downgrading of different types of coastal wetlands. Such information can help guide effective and targeted coastal wetland conservation, management, and restoration measures.

* Corresponding author.
E-mail address: wenhong.li@duke.edu (W. Li).

http://dx.doi.org/10.1016/j.scitotenv.2023.164995
Received 14 March 2023; Received in revised form 9 June 2023; Accepted 16 June 2023
Available online 19 June 2023

1. Introduction

Coastal wetlands provide critical ecosystem services that aid in regulating and mitigating climate change (MEA, 2005; McLeod et al., 2011). However, these valuable ecosystems have been experiencing intensified disruptions from human activities and climate change in recent years. Sea-level rise (SLR) (Blankespoor et al., 2014; Spencer et al., 2016; Schuerch et al., 2018), frequent extreme weather events (Tahsin et al., 2016), and anthropogenic activities (Cloern et al., 2016; Church and White, 2011; Dangendorf et al., 2017; He and Silliman, 2019) individually or combined can result in widespread wetland downgrading. In this study, wetland downgrading is defined as the loss of wetland area or reduction in wetland vegetation coverage and biomass due to altered environmental conditions, and the ecosystem cannot recover to its original state if environmental constraints persist (He et al., 2022; Wessels et al., 2016; Grenfell et al., 2007; Shen et al., 2019; Smart et al., 2020). The former refers to an area changing from wetland to non-wetland (Wessels et al., 2016), while the latter indicates the wetland's conversion from a relatively structurally complex and multi-layered wetland type to a wetland type with simpler vegetation structure and reduced biomass (e.g., woody wetlands converting into emergent herbaceous wetlands, i.e., the formation of "ghost forests") (Grenfell et al., 2007; Kirwan and Gedan, 2019; Senter, 2003; Shen et al., 2019; Smart et al., 2020). Substantial wetland downgrading often leads to a long-term reduction in vegetation coverage, a shift in dominant vegetation types, and fragmentation of the landscape (Aguilos et al., 2022; He et al., 2022; Hu et al., 2020; Smart et al., 2020; Ury et al., 2021). Massive coastal wetland loss and emergences of ghost forests have been observed and documented along the North Atlantic Coast and the Gulf of Mexico in recent decades (Kirwan and Gedan, 2019; Smart et al., 2020).

Coastal wetland ecosystems often consist of woody wetlands and emergent herbaceous wetlands (Dewitz, 2021; Zhang et al., 2018, 2019). Due to their various vegetation composition and structures, different types of wetlands have different resilience to external stresses. For example, it was found that rising sea levels could not only cause emergent herbaceous wetland losses by inundating marshes but also pose stresses on woody wetlands and lead to the formation of ghost forests by elevating saltwater tables (SWT) along the North American Atlantic and Gulf of Mexico coasts (He et al., 2022; Kirwan and Gedan, 2019; Senter, 2003). Ellison (1999) demonstrated that hurricanes could lead to the death of mangroves by smothering their roots with excess sediment on the surface while Morton and Barras (2011) and Yu et al. (2016) indicated that hurricanes could impact marshes through prolonged retention of saline storm-surge water and increased marsh salinization. These studies suggested that climatic disturbances lead to wetland downgrading mainly through changing their hydrogeomorphic conditions, making them unfavorable for vegetation survival. They also implied that the driving factors of wetland destruction vary substantially for different wetland types. However, what are the most crucial hydrogeomorphic variables/drivers for different types of coastal wetlands and what are their critical thresholds have not been systematically and quantitatively investigated, especially on large scales. Such knowledge is essential for optimizing wetland conservation and restoration planning.

Most existing studies assessing the drivers of wetland downgrading use conventional regression models. The majority of these regression models require prior assumptions about the relationships (such as linear or logistic relationships) between environmental variables and wetland changes. Furthermore, these studies focused on one single type of downgrading, mostly the loss of salt marsh (Cui et al., 2014; Kirwan and Megonigal, 2013; Schieder et al., 2018; Stagg et al., 2020). For example, Stagg et al. (2020) quantified elevation thresholds on marsh fragmentation in coastal wetlands of the Chenier Plain along the Northern Gulf of Mexico using a sigmoidal regression model. Based on multivariate logistic regression models, Cui et al. (2014) analyzed the driving forces causing declines in marsh wetland landscapes in the Honghe region, northeast China. An issue with traditional regression models stems from the fact that determining the prior assumptions about the linkages between environmental variables and wetland changes requires existing knowledge, prior experience, and extensive wetland research (Sutula et al., 2006). In addition, the relationships may be too complex and challenging to be fitted by explicit mathematical functions. To avoid these issues, machine learning methods have emerged in recent years to detect the relationships between driving factors and coastal wetland changes across different types of wetlands (Gray et al., 2021; Mutanga et al., 2012).

Unlike conventional regression methods, machine learning models do not need prior assumptions regarding the relationships between predictors and the response variable (Belmokre et al., 2019; Carranza et al., 2021; Gao, 2018; Maxwell et al., 2016). Machine learning methods, such as support vector machine (SVM), k-nearest neighbors (K-NN), artificial neural network (ANN), decision tree (DT), and random forest (RF), have been demonstrated to be more accurate and efficient when applied to high-dimensional, correlated, and large-volume data spaces (Abbasian et al., 2022; Maxwell et al., 2016; Zhang et al., 2021a). For example, Wu et al. (2017) established a RF progression model to study the driving forces of wetland density changes in the western Liaohe river basin. They found that among the five influencing factors (elevation, slope, temperature, precipitation, and population density), precipitation dominated changes in the wetland density. Using ANN, SVM, and the maximum likelihood method, Kesikoglu et al. (2019) quantified land use and land cover (LULC) changes at the Sultan Marshes wetland, Turkey.

Among these machine learning algorithms, the random forest (RF) model is found to be more efficient in analyzing the combined effects of disturbances and identifying the predominant driving factors for LULC changes (Souza et al., 2020; Wessels et al., 2016; Wu et al., 2017; Zhang et al., 2021a; Zhang et al., 2021b; Zhu and Woodcock, 2014). For instance, Zhang et al. (2021a) assessed the performance of four machine learning models, including SVM, RF, K-NN, and ANN, in detecting hurricane-caused forest damage. Their study indicated that the RF has the highest overall accuracy. In addition, RF models possess the capability to effectively assess the relative importance of each driver in determining the response variable (Flanagan and Richardson, 2010; Rohmer et al., 2018; Shiroyama and Yoshimura, 2016; Tesoriero et al., 2017). Furthermore, RF models can elucidate how the response variable changes with driving forces by calculating partial dependence between them (Huang et al., 2021; Long et al., 2017). As a result, RF models have become one of the extensively used machine learning algorithms for LULC analysis (Breiman, 2001; Peltola et al., 2019; Sulova and Arsanjani, 2021). However, it has been rarely applied to understand the transformation drivers of wetland ecosystems, especially coastal wetlands.

This study aims to assess the relative importance of various hydrogeomorphic forcing factors contributing to the downgrading of coastal wetlands, including woody and emergent herbaceous wetlands, and identify the key factor(s) by using the RF classification models. To the best of our knowledge, this is the first attempt to thoroughly study the driving factors of different types of coastal wetland downgrading using RF models. In addition to RF models, a hydrological model, PIHM-Wetland, was also used in this study (He et al., 2022; Zhang et al., 2018, 2019, 2022a) due to the lack of extensive and long-term monitoring of key hydrological variables (e.g., groundwater tables (GWT) and saltwater tables (SWT)). The PIHM-Wetland model has been proven effective in simulating regional-scale hydrological processes (e.g., GWT, SWT, and overland flow) across environmental gradients and has already been well-calibrated and validated for the study domain (He et al., 2022; Zhang et al., 2018, 2019, 2022a). The objectives of this study are to (1) use RF models to investigate the relative importance of different hydrogeomorphic variables on three different types of wetland downgrading, including woody wetland loss, emergent herbaceous wetland loss, and woody wetland downgrading to emergent herbaceous wetlands; and (2) quantify the critical threshold of the dominant hydrogeomorphic factor driving wetland downgrading. By examining the relationships between hydrogeomorphic variables and coastal wetland downgrading, we demonstrate how climate change, saltwater intrusion due to sea-level rise (SLR), and anthropogenic activities (such as wetland drainage) impact the valuable coastal wetlands. Under intensified climate change especially accelerating SLR, combining machine learning models with hydrological modeling provides new opportunities to better assess the impacts of climate change on coastal wetland ecosystems on regional scales (Masson-Delmotte et al., 2021; Oppenheimer et al., 2019; Sallenger et al., 2012; Wen and Hughes, 2020).

2. Material and methods

2.1. Study area

The study area is located in the southeast part of the Alligator River National Wildlife Refuge (ARNWR) in Dare County, North Carolina (NC), USA, with an area of ~400 km^2 (Fig. 1a). 96 % of the study area is coastal wetlands, with most emergent herbaceous wetlands (15 %) along the coastline and woody wetlands (81 %) distributed landward (Moorhead and Cook, 1992). Evergreen forests (50 %) and mixed forests (50 %) make up the majority of vegetation types in woody wetlands, which include loblolly pine (*Pinus taeda L.*), pond pine (*Pinus serotina Michx.*), sweetbay magnolia (*Magnolia virginiana L.*), and red bay (*Persea borbonia (L.) Spreng.*) (Richardson, 2012). Marshes (60 %) and shrubs (40 %) constitute emergent herbaceous wetlands (He et al., 2022; Moorhead and Brinson, 1995; Zhang et al., 2019) with typical vegetation communities including sawgrass (*Cladium jamaicense*), black needlerush (*Juncus roemerianus Scheele*), and panic grasses (*Panicum* spp.) (U.S. Fish & Wildlife Service, Washington, DC, U.S.A., https://www.fws.gov/refuge/Alligator_River/). The limited number of inlets between barrier islands connecting the sounds to the ocean creates a gradient in salinity from the moderate salinity (10–18 ppt) in Pamlico Sound in the south to the primarily freshwater (< 5 ppt) in Albemarle Sound in the north (Fig. 1a) (Kemp et al., 2009; Wells and Kim, 1989). And the tide range is low, which is 10 cm or less throughout most of the study area (Wells and Kim, 1989).

In the mid-20th century, this area was extensively drained for agriculture and forestry, resulting in a dense network of ditches and canals across the landscape (approximately 4 km of drainage length per square-kilometer area) (Poulter, 2005). Coupled with its low elevation (< 1 m) and gentle slope (almost flat), the area was found to have little surface/subsurface freshwater input but significant saltwater intrusion inland through ditches and canals that connect directly or indirectly to the estuarine shoreline (Smart et al., 2020; Ury et al., 2021; Wells and Kim, 1989). Increased soil salinization and inundation have caused changes in land cover. Large areas of emergent herbaceous wetlands were converting to open water. In addition, freshwater-dependent coastal woody wetlands were retreating, leaving behind dead trees surrounded by salt-tolerant shrubs, herbaceous plant species, and/or open water (Hackney and Yelverton, 1990; He et al., 2022; Williams et al., 1999). These wetland losses and the formation of ghost forests are commonly seen along the east coast of the USA in recent years (Fagherazzi et al., 2019; Kirwan and Gedan, 2019; Senter, 2003; Smart et al., 2020; Ury et al., 2021; Wasson et al., 2013).

2.2. Methods

To investigate the relative importance of multiple coastal hydrogeomorphic variables contributing to coastal wetland downgrading in the ARNWR and identify the dominant driver, we implemented the random forest (RF) classification models on wetlands that downgraded during 1995–2019 as identified by He et al. (2022). Potential driving variables include elevations, distance to canals/ditches, the maximum seasonal saltwater and groundwater table (SWT_{max} and GWT_{max}), and the percentage of inundation time (PIT). Due to the density difference between saltwater and freshwater, saltwater usually exists beneath fresh groundwater forming a saltwater-freshwater interface (Gupta, 1985; Polo and Ramis, 1983; Shamir and Dagan, 1971). Therefore, in this study, the saltwater table (SWT) refers to the depth from the ground surface to the saltwater-freshwater interface. In contrast, the groundwater table (GWT) refers to the depth from the ground surface to the top of the saturated zone. Negative (positive) GWT/SWT represents the GWT/SWT below (above) ground. In the RF models, whether or not wetland ecosystems downgraded serves as the response variable (see Section "2.2.1 Response variables" for details) and the potential driving variables act as explanatory variables (a.k.a. predictors, see Section "2.2.2 Predictors" for details).

2.2.1. Response variables

Response variables for RF models in this study are downgraded and non-downgraded wetlands identified by He et al. (2022). By analyzing fine-scale and long-term Landsat-derived Normalized Difference Vegetation Index

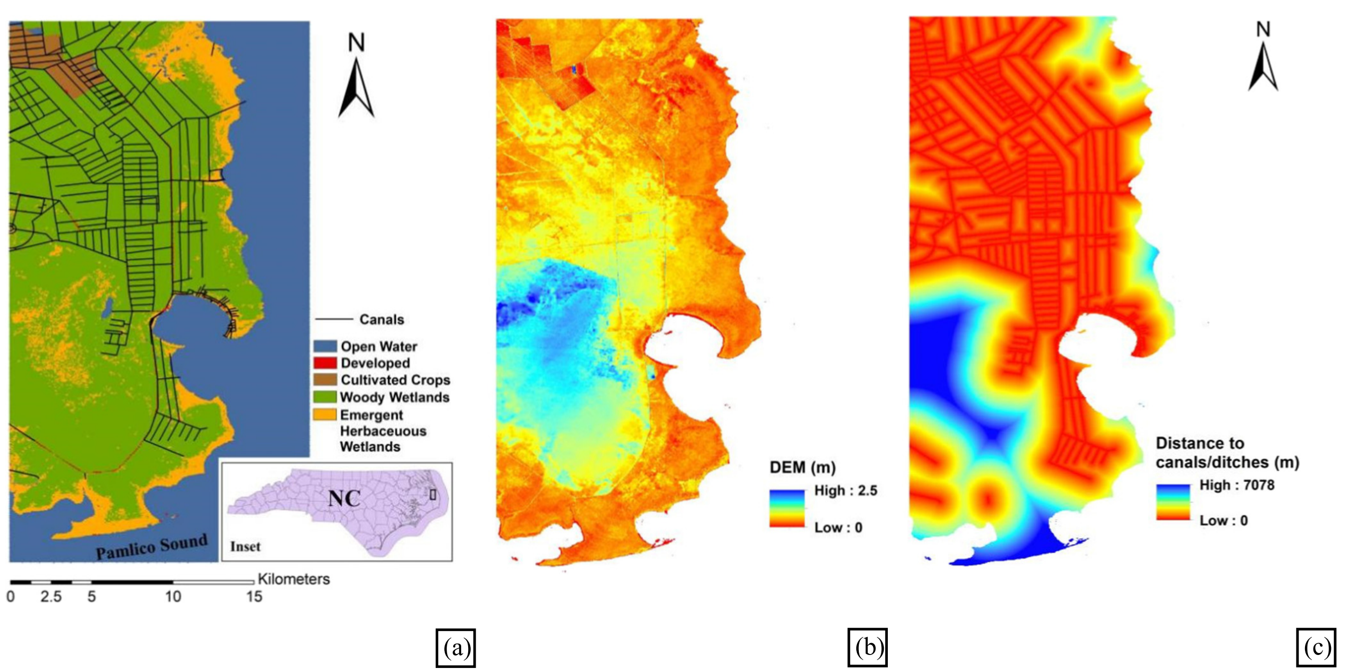

Fig. 1. (a) Study area (35.558–35.863°N, 75.693–75.859°W, excluding Open Water) with land cover types (adapted from 2019 National Land Cover Database (NLCD)) and canals/ditches (from the National Hydrography Dataset). The location of Pamlico Sound is shown, while Albemarle Sound is north of the study area and beyond the area shown here. Inset: the location of the study area (black box) in North Carolina (NC), USA. (b) Spatial patterns of elevation (the digital elevation model (DEM), unit: m). (c) Spatial patterns of the distance to canals/ditches (unit: m).

(NDVI) time series, He et al. (2022) identified the spatial and temporal patterns (downgrading locations and years) of 3569 ha of wetland downgrading over the study area during 1995–2019, which includes woody wetland loss, emergent herbaceous wetland loss, and woody wetlands downgrading to emergent herbaceous wetlands (Fig. 2). Existing studies suggested that emergent herbaceous wetlands and woody wetlands may have different capacities to withstand stressful hydrological conditions due to their dissimilar vegetation composition and structures (He et al., 2022; Kirwan and Gedan, 2019; Schieder et al., 2018), thus, two RF classification models are needed. One RF model is used for woody wetlands (RF1) to discriminate downgraded woody wetlands (DW) from non-downgraded woody wetlands (NDW, Fig. 2a), and the other for the emergent herbaceous wetlands (RF2) to separate downgraded emergent herbaceous wetlands (DH) from non-downgraded emergent herbaceous wetlands (NDH, Fig. 2b). The binary response variable is denoted as "1" if the area is downgraded, i.e., DW and DH; it is "0" for non-downgraded wetlands, including NDW and NDH (Supplementary Table S1). In addition, because woody wetlands can downgrade into either emergent herbaceous wetlands or non-vegetated areas (Fig. 2c), we fit the third RF model, i.e., RF3, to differentiate woody wetlands downgrading to non-vegetated areas (W2N) from woody wetlands downgrading to emergent herbaceous wetlands (W2H); in this case, the response variable is denoted as "11" and "10" for the two types of downgrading, W2N and W2H, respectively (Supplementary Table S1).

2.2.2. Predictors

Previous research found that disturbances/drivers result in wetland downgrading mainly through altering their hydrogeomorphic processes (Conner et al., 2002; Day et al., 2008; Rodríguez-Iturbe and Porporato, 2007; Williams et al., 2003; Winter, 2000; Zhang et al., 2018, 2019, 2022a), we thus chose the following hydrological and topographic variables (collectively referred to as "hydrogeomorphic variables") that control coastal wetland hydrogeomorphic dynamics as predictors: elevations, distance to canals/ditches, the maximum seasonal saltwater table (SWT_{max}), the maximum seasonal groundwater table (GWT_{max}), and the percentage of inundation time (PIT).

Stagg et al. (2020) showed that the fragmentation of marshes along the Northern Gulf of Mexico was primarily controlled by elevation. Thus, we extracted the elevation variable (the digital elevation model (DEM), Fig. 1b) from the Coastal National Elevation Database (CoNED) Applications Project with a spatial resolution of 1 m (Danielson et al., 2016, 2018; Irwin et al., 2021). Fig. 1b illustrates that about 73 % of the study area is below 1 m above sea level, with lower elevations along the coastline and higher elevations landward.

Besides the DEM, the distance to canals/ditches for each grid (Fig. 1c) was also calculated because artificial drainage networks can serve as conduits for saltwater intrusion if connected to the estuarine shoreline (Smart et al., 2020; Ury et al., 2021). Here we used the National Hydrography Dataset ([dataset] U.S. Geological Survey, National Hydrography Dataset, accessed on 7 May 2021, https://www.usgs.gov/national-hydrography/national-hydrography-dataset) to identify canals/ditches that were directly or indirectly (connected via other canals/ditches) connected to the estuarine shoreline. Then the Euclidean distance from the center of each grid to its nearest canal/ditch was calculated.

In addition to topographic variables (DEM and distance to canals/ditches), three hydrological variables (SWT_{max}, GWT_{max}, and PIT) were investigated to capture the changes in hydrological processes critical to wetland downgrading (He et al., 2022; Mitsch and Gosselink, 2015; Rodríguez-Iturbe and Porporato, 2007; Zhang et al., 2018, 2019, 2022a). The maximum seasonal saltwater table (SWT_{max}) quantifies the extent of saltwater intrusion while the maximum seasonal groundwater table (GWT_{max}) reflects the flooding and drought conditions. The seasonal SWT and GWT were aggregated from the PIHM-Wetland simulated daily SWT and GWT. Then, we calculated SWT_{max} and GWT_{max} for downgraded and non-downgraded wetland grids. For downgraded grids, we hypothesized that extreme SWT and GWT in the year of wetland downgrading most likely contributed to the occurrence of wetland downgrading, therefore, we derived SWT_{max} and GWT_{max} as the maximum values of seasonal SWT and GWT in the year of downgrading; for the grids without experiencing downgrading, SWT_{max} and GWT_{max} were derived as the maximum values of seasonal SWT and GWT during the entire study period (1995–2019) as

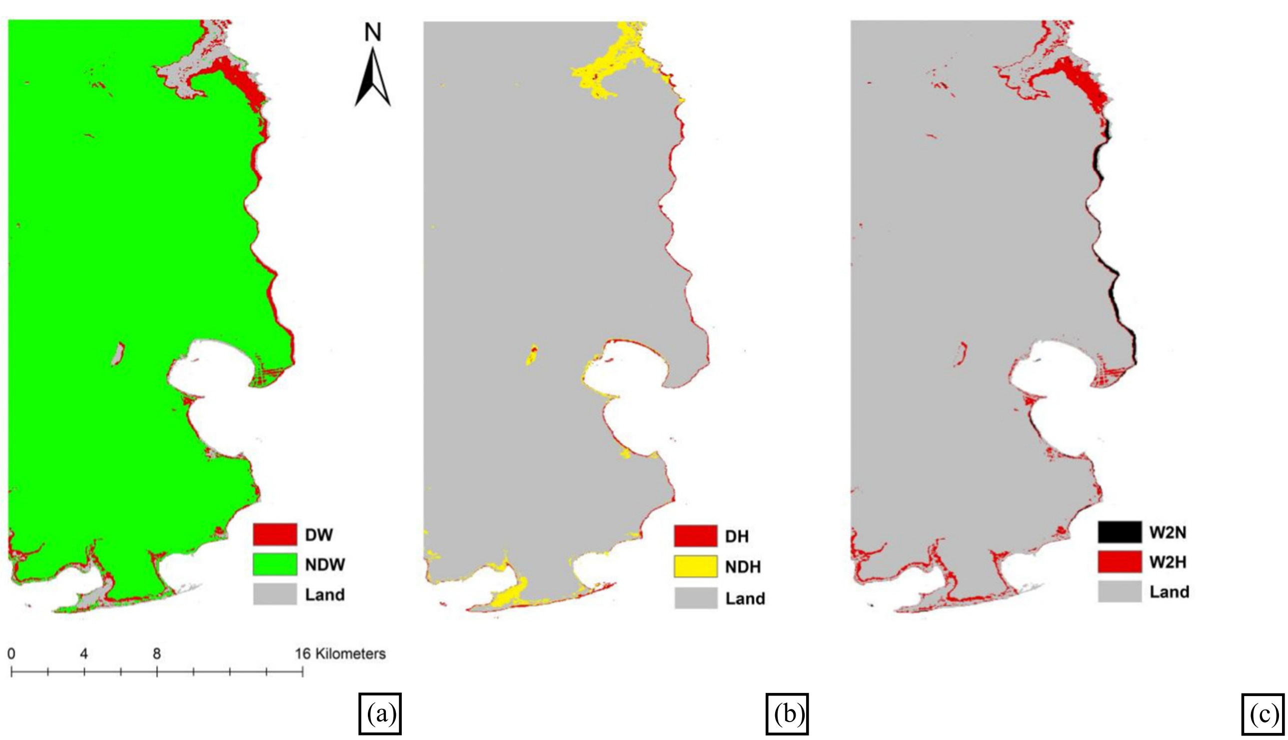

Fig. 2. Spatial distribution of (a) downgraded and non-downgraded woody wetlands (DW and NDW), (b) downgraded and non-downgraded emergent herbaceous wetlands (DH and NDH), and (c) woody wetlands downgrading to emergent herbaceous wetlands or non-vegetated areas (W2H or W2N) over the study area identified by He et al. (2022).

these non-downgraded wetlands are not sensitive to the seasonality and extremes of SWT and GWT. The percentage of inundation time (PIT) was calculated as Eq. (1) to estimate the inundation's impact:

$$\text{Percentage of inundation time (PIT)} = \frac{N_{GWT \geq 0}}{N} \quad (1)$$

where $N_{GWT \geq 0}$ was the number of days when daily GWT was greater than or equal to 0, and N was the total number of days in the downgrading year and the entire study period (1995–2019) for downgraded and non-downgraded grids, respectively. Given that wetland downgrading spots (response variables) were identified based on remote sensing grids with a 30-m spatial resolution (He et al., 2022), all predictors were derived at or resampled to a spatial resolution of 30 m. The resampling process was conducted in ArcMap 10.5.1 using the "Resample" function (Resampling Technique: NEAREST) under the "Data Management" Tool (ArcGIS, 2016).

Here, we showed an example of deriving three hydrological variables, SWT_{max}, GWT_{max}, and PIT, for a randomly selected grid within ARNWR. Fig. 3 illustrates the seasonal variations of the NDVI, SWT, and GWT at the grid from 1995 to 2019. In the summer of 2010, the selected wetland grid changed from an emergent herbaceous wetland to a non-vegetated area (please refer to He et al. (2022) for details); thus, SWT_{max} and GWT_{max} were derived as the maximum values of seasonal SWT and GWT in the year 2010, i.e., 0.21 m and 0.35 m, respectively. In addition, PIT was calculated as the number of inundated days in 2010, i.e., PIT = 1, since GWT was larger than zero for all 365 days in 2010. Also using different reasonable time intervals (e.g., a two-year period) to derive these hydrological variables—SWT_{max}, GWT_{max}, and PIT—for the downgraded wetland grids did not change the overall results of the RF models (not shown).

2.2.3. Random forest classification models

In this study, three RF classification models were fitted to investigate the relative importance of different driving factors of three types of wetland downgrading: DW or NDW (RF1), DH or NDH (RF2), and W2N or W2H (RF3), respectively (Supplementary Table S1). Each RF model includes many classification trees constructed from bootstrapped training data samples (Hikouei et al., 2021). The output of the RF classification model is calculated by plurality votes of the RF's classification trees (Breiman, 2001). As a result, the RF method employs the bootstrap aggregation (bagging) technique and fully exploits ensembles to reduce classification errors (Breiman, 2001). Furthermore, the predictors (i.e., the five hydrogeomorphic variables) used in split nodes are chosen from a random sample of all predictors to minimize the probable correlation across trees in the forest and reduce the potential of over-fitting (Breiman, 2001; Hikouei et al., 2021; Peltola et al., 2019). See Section S2 in the supplementary for details on the hyperparameter values used in each random forest model.

The RF classification model can quantitatively assess each explanatory variable's contribution to the classification results (Sulova and Arsanjani, 2021). Based on the values of the contribution (Gini importance), we quantified and ranked the relative importance of the forcing variables on wetland downgrading. The variable with the highest Gini importance value was considered "the dominant driver". Furthermore, the RF algorithm can explicitly mine the relationships between explanatory variables and the response variables by computing the partial dependence between them (see Section "2.2.6 Partial dependence"; Peng et al., 2020; Strobl et al., 2008), which allows us to not only distinguish the dominant driver key to the wetland downgrading but also quantify the relationships between the key hydrogeomorphic variable and the response variable (DW or NDW, DH or NDH, and W2N or W2H).

2.2.4. Training and testing dataset preparation

To test the performance of the RF models, the popular machine learning validation method, train and test, was adopted. However, before splitting the data into training and testing datasets, we noticed that the data were highly imbalanced. Specifically, the number of non-downgraded/slight-downgraded grids, including NDW (413,913), NDH (11,640), and W2H (13,219) (with the response variable denoted as "0" or "10", Supplementary Table S1), is about 20 times greater than the number of downgraded/severe-downgraded grids—DW (15,404), DH (3888) or W2N (2185) (with the response variable denoted as "1" or "11", Supplementary Table S1). The imbalanced numbers of downgraded/severe-downgraded and non-downgraded/slight-downgraded grids may result in poor classification performance of the RF models (Shearman et al., 2019). The poor performance is because the RF models can achieve high overall accuracy scores by simply labeling each grid as the majority class (NDW or NDH or W2H with the response variable denoted as "0" or "10",

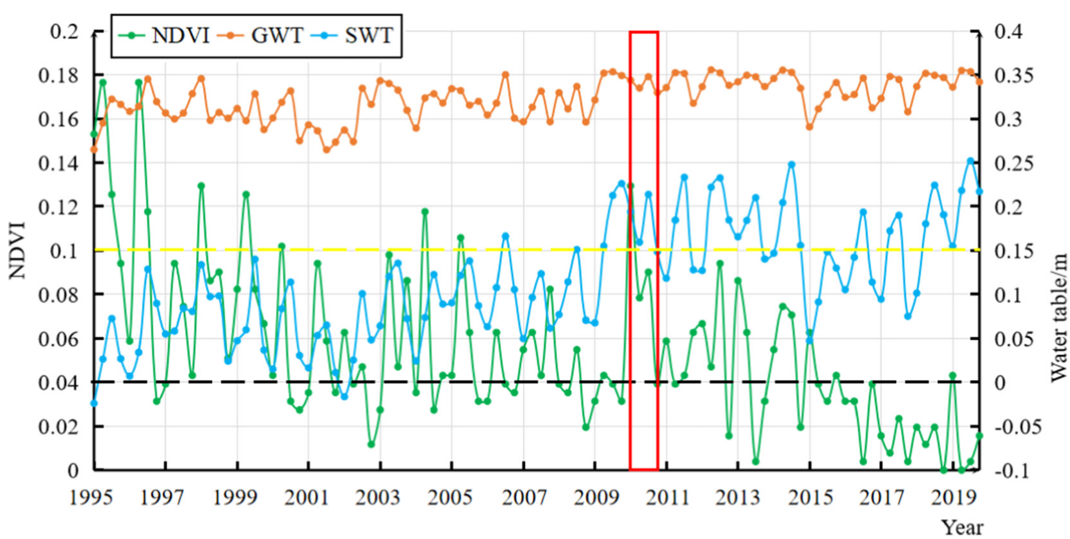

Fig. 3. Time series of the seasonal Normalized Difference Vegetation Index (NDVI; green, left y-axis), saltwater tables (SWT; blue, right y-axis), and groundwater tables (GWT; orange, right y-axis) for a randomly selected grid within the study area during 1995–2019. The horizontal black dashed line delineates the land surface; The yellow dash line represents the lower boundary of NDVI value for the emergent herbaceous wetland, below which means the wetland has converted to a non-vegetated area. Downgrading happened in 2010 (red box, i.e., NDVI dropped from 0.18 in 1995 to 0.09 in 2010 and never came back, see He et al. (2022) for details). The maximum seasonal saltwater and groundwater table (SWT_{max} and GWT_{max}) were thus calculated as the maximum values of seasonal SWT and GWT in 2010 for the downgraded wetland grid, i.e., 0.21 m and 0.35 m for SWT_{max} and GWT_{max}, respectively. The percentage of inundation time (PIT) was calculated as the number of inundated days ($GWT \geq 0$) in the year 2010 for the grid.

Supplementary Table S1). However, the model fails to capture the minority class (DW or DH or W2N with the response variable denoted as "1" or "11", Supplementary Table S1). This problem is common in machine learning, especially in classifications (Feng et al., 2020; Robinson et al., 2018; Wen and Hughes, 2020). To address this issue, before splitting the paired data into the training and testing datasets, we over-sampled the minority category (Mohammed et al., 2020). Specifically, we first separated the samples of each category into two different data frames based on their response variables ("0" versus "1" or "10" versus "11"). Next, we used the replacement sampling method (Raj and Khamis, 1958) to resample the minority category so that the number of samples could equal the number of samples in the majority category. Finally, we merged the over-sampled minority-category data frame with the original majority-category data frame. The new merged data frame has the same number of datasets labeled as "0" and "1" or "10" and "11" and can be utilized for creating the training and testing datasets (Supplementary Table S1). The new data frame was split with a ratio of 75/25 for training and testing purposes, respectively (Bayley and Falessi, 2018; Santoso et al., 2017). Consequently, RF1 was trained using a 75 % training dataset including 620,869 samples, which contained 310,550 NDW grids and 310,319 DW grids. The training dataset for RF2 had 17,460 samples, including 8733 NDH grids and 8727 DH grids. For RF3, 19,828 samples consisting of 9885 W2H grids and 9943 W2N grids were used for training (Supplementary Table S1).

2.2.5. Model evaluations

To assess the performance of the trained RF models, we fed the explanatory variables of the testing datasets (25 % of the total data) into trained RF models. Then, results from the RF classification models were compared with the corresponding response variables of the testing datasets. Five metrics were employed to quantify the accuracy of the models: confusion matrix, overall accuracy, omission and commission errors, and the kappa statistic.

The confusion matrix summarizes classification results for a category in which the number of correct and incorrect classifications are counted by category (Stehman, 1997). The percentage of correctly classified results in the confusion matrix is referred to as overall accuracy (Stehman, 1997), which can be calculated in percentages as stated in Eq. (2):

$$\text{Overall Accuracy} = \frac{\mathrm{TP} + \mathrm{TN}}{\mathrm{TP} + \mathrm{TN} + \mathrm{FN} + \mathrm{FP}} \times 100\% \tag{2}$$

where TP and TN are the grid number of true positive and negative classifications, separately; FP and FN represent numbers of false positive and negative classifications, respectively (Stehman, 1997). For each class i, the percentage of reference grids that were left out (or omitted) from the correct class i in the classification out of the total number of reference grids in class i and the percentage of grids that were incorrectly classified as class i out of the total number of classified grids in class i are referred to as the omission and commission errors, separately (Ackoff, 1994).

Kappa statistic, another widely used accuracy assessment metric, reveals as a more effective evaluator because of taking into account the prior probability of the response variable (Cohen, 1960). It compares an observed accuracy with a random chance and can be calculated as

$$\mathrm{kappa}(\mathrm{k}) = \frac{\mathrm{P_o} - \mathrm{P_e}}{1 - \mathrm{P_e}} \tag{3}$$

where P_o is the overall accuracy, and P_e is the theoretical probability of chance agreement, using the observed data to calculate the probabilities of randomly seeing each category (Cohen, 1960).

2.2.6. Partial dependence

The partial dependence between the dominant driver and the response variable was calculated to investigate how the most critical predictor influenced coastal wetland ecosystems. Defined as the dependence of the downgrading probability on a predictor after averaging out the effects of the other predictors in the RF model (Cutler et al., 2007; Friedman, 2001; Hastie et al., 2001), high (low) partial dependence suggests a high (low) probability of DW/DH/W2N occurring (Zeng et al., 2017). As the calculation of the partial dependence requires variables to be independent of one another, Pearson correlations between each explanatory variable were calculated first to filter independent predictors (Supplementary Fig. S1). Then, the Partial Dependence Plot (PDP) was made to understand changes in the probability of coastal wetland downgrading in response to the critical driver. The formula of the PDP is given in Eq. (4):

$$\mathrm{f}(\mathrm{X_i}) = \frac{1}{\mathrm{n}} \sum_{\mathrm{k}=1}^{\mathrm{n}} \mathrm{RF}\left(\mathrm{x_1^k}, \ldots, \mathrm{x_i}, \ldots, \mathrm{x_m^k}\right) \tag{4}$$

where x_i^k represents the kth sample of the ith independent predictor, m represents the number of predictors, n represents the number of samples, and RF(·) represents the re-trained RF models only based on independent predictors (see Supplementary Tables S3 and S4, Fig. S1) (Friedman, 2001; Hastie et al., 2001).

3. Results

3.1. Accuracy assessment of the random forest classification models

Evaluation metrics calculated on the testing datasets demonstrate that the RF1 and RF2 models can well distinguish downgraded wetlands from non-downgraded wetlands and that RF3 accurately classifies W2N from W2H (Table 1). The overall accuracy of the three RF models is 99.7 % (RF1), 97.1 % (RF2), and 97.6 % (RF3), respectively. The errors of omission and commission are 0 % and 0.5 % for the DW class (RF1), 1.3 % and 3.5 % for the DH class (RF2), and 0.5 % and 5.1 % for the W2N class (RF3), separately. The three RF models' kappa statistics had similar patterns to the overall accuracy, with the RF1 model achieving the highest kappa statistic (0.99) and the RF2 model having the lowest kappa statistic (0.94).

The confusion matrix also reveals that the three RF models classified well as the numbers of TP and TN were far more than those of FP and FN (Table 1). The RF1 model correctly classified all the downgrading samples in the testing dataset (103,594 of 103,594, 100 %). 99.5 % of samples of NDW (102,812) were properly classified with the omission error only being 0.5 % and the commission error being 0 %. The RF2 model successfully labeled 96.4 % of NDH testing samples (2802 of 2907). It also accurately allocated 98.7 % of DH testing samples (2876 of 2913) and only omitted 37 (the omission error being 1.3 %) DH testing samples. The RF3 model also performed well with the correct classification of 94.7 % W2H testing samples (3158 of 3334) and 99.5 % W2N testing samples (3259 of 3276).

The stability of RF models was also validated. The train/test split approach with a ratio of 75/25 was utilized in this study as the most frequent form of validation (Moon et al., 2018; Pawluszek-Filipiak and Borkowski, 2020). Other commonly used train/test split ratios (e.g., 80/20 or 70/30) did not significantly affect the performance of the RF models (not shown). Furthermore, the training/testing samples were generated at random, which should mitigate the risk of sampling bias and assure the results be meaningful (Perry and Dickson, 2018).

3.2. Key variables contributing to wetland downgrading

Fig. 4 shows the importance analysis of predictors in the three coastal wetland downgrading scenarios. The analysis suggests that several disruptions/changes in hydrogeomorphic processes collectively contribute to the loss/downgrading of coastal wetland ecosystems. However, Fig. 4 also suggests that the dominant driver varies for different types of wetland downgrading. Specifically, the most crucial variable for the woody wetland downgrading was $\mathrm{SWT_{max}}$ (Fig. 4a), with a Gini importance value of 0.3, higher than the Gini importance values of other predictors. The distance to canals/ditches emerges as the predominant factor in determining the final fates of downgraded woody wetlands (Fig. 4c): either the woody wetland downgraded to the emergent herbaceous wetland (W2H) or lost the vegetation (W2N). Fig. 4b shows that elevation (DEM) played an essential

Table 1
Overall statistics of the accuracy assessment results of the three RF models.

RF models	Categories	Confusion Matrix		Overall Accuracy (%)	Omission error (%)	Commission error (%)	Kappa
		Classified grids without downgrading or W2H	Classified grids experiencing downgrading or W2N				
RF1: Downgraded and Non-downgraded Woody Wetlands	Observed NDW grids	102,812	551	99.7	0.5	0	0.995
	Observed DW grids	0	103,594		0	0.5	
RF2: Downgraded and Non-downgraded Emergent Herbaceous Wetlands	Observed NDH grids	2802	105	97.6	3.6	1.3	0.951
	Observed DH grids	37	2876		1.3	3.5	
RF3: Downgraded Woody Wetlands	Observed W2H grids	3158	176	97.1	5.3	0.5	0.942
	Observed W2N grids	17	3259		0.5	5.1	

role in emergent herbaceous wetland downgrading. Interestingly, PIT was the least important variable in the three RF models (Fig. 4).

Fig. 5 shows the partial dependence plot (PDP) of the most important predictors for the three RF models. A sigmoidal response of downgrading probability to SWT_{max} exists in the coastal woody wetlands, with -0.8 and $-$ 0.2 m being the lower and upper thresholds, respectively (Fig. 5a). This result indicates that SWT_{max} below the land surface by 0.2–0.8 m is critical to woody wetlands, where a miniature rise of SWT_{max} would cause a disproportionate increase in the probability of woody wetland downgrading. When SWT_{max} reaches 0.2 m below the surface or higher, the woody wetlands have a high probability of downgrading.

Fig. 5b demonstrates a non-linear relationship between DEM and the likelihood of emergent herbaceous wetland downgrading. DEM higher than 0.7 m or lower than 0 m significantly increased the probability of downgrading for the emergent herbaceous wetlands. In this coastal area, GWT_{max} was significantly negatively correlated with DEM (Fig. 6; R^2 = 0.81, $p < 0.0001$), suggesting that emergent herbaceous wetlands with high DEM were associated with low GWT_{max} and thus more vulnerable to droughts, while those with low DEM were found to have high GWT_{max} and therefore were more susceptible to floods. Quantitatively, the relationship between DEM and GWT_{max} could be well fitted linearly as $GWT_{max} = -0.95 \times DEM + 0.34$ (Fig. 6). Thus, 0.34 m above the land surface

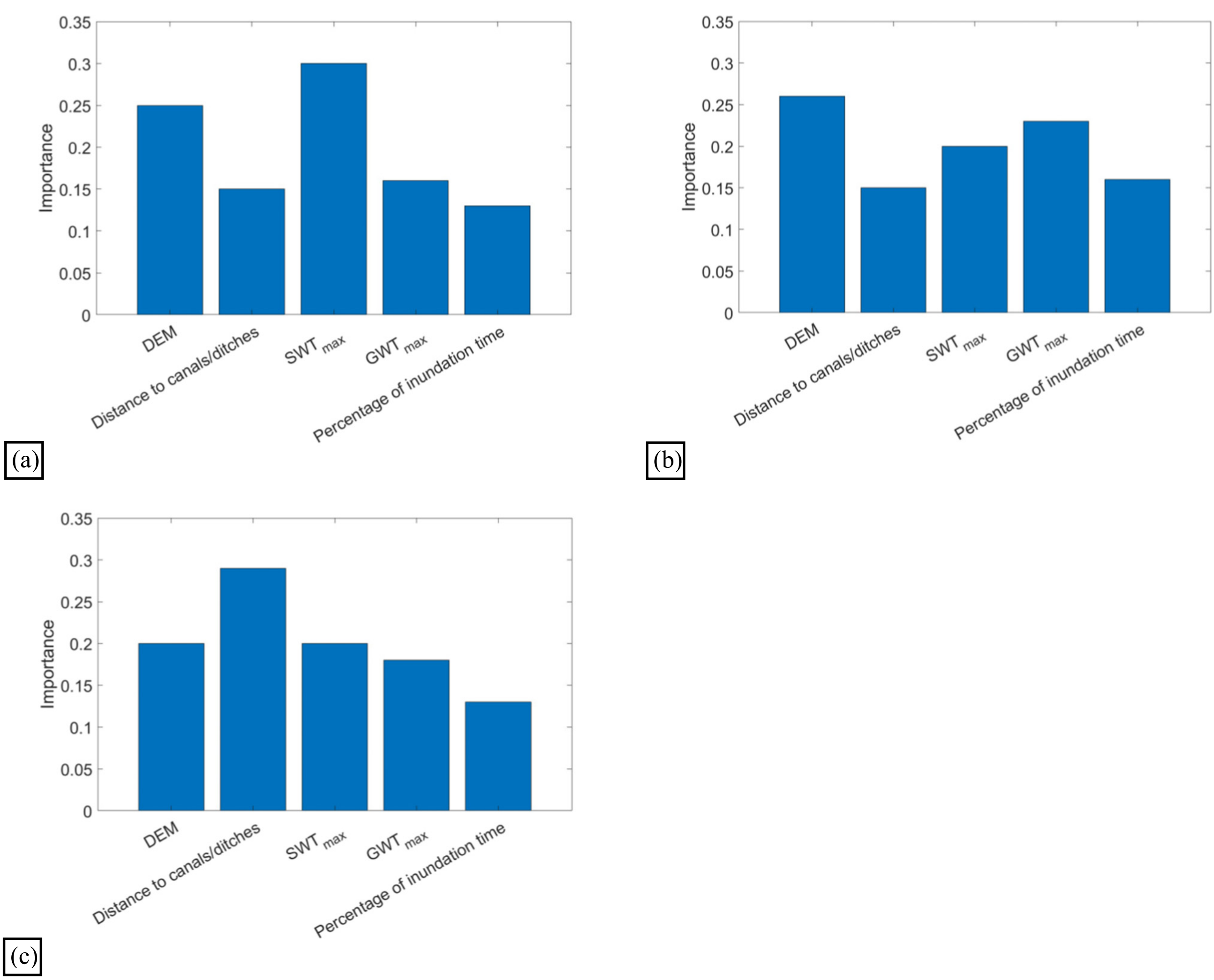

Fig. 4. The variable importance analysis in the three random forest (RF) models. (a) RF1: DW and NDW, (b) RF2: DH and NDH, and (c) RF3: W2N and W2H. DEM represents the digital elevation model. SWT_{max} and GWT_{max} stand for the maximum seasonal saltwater and groundwater tables, respectively.

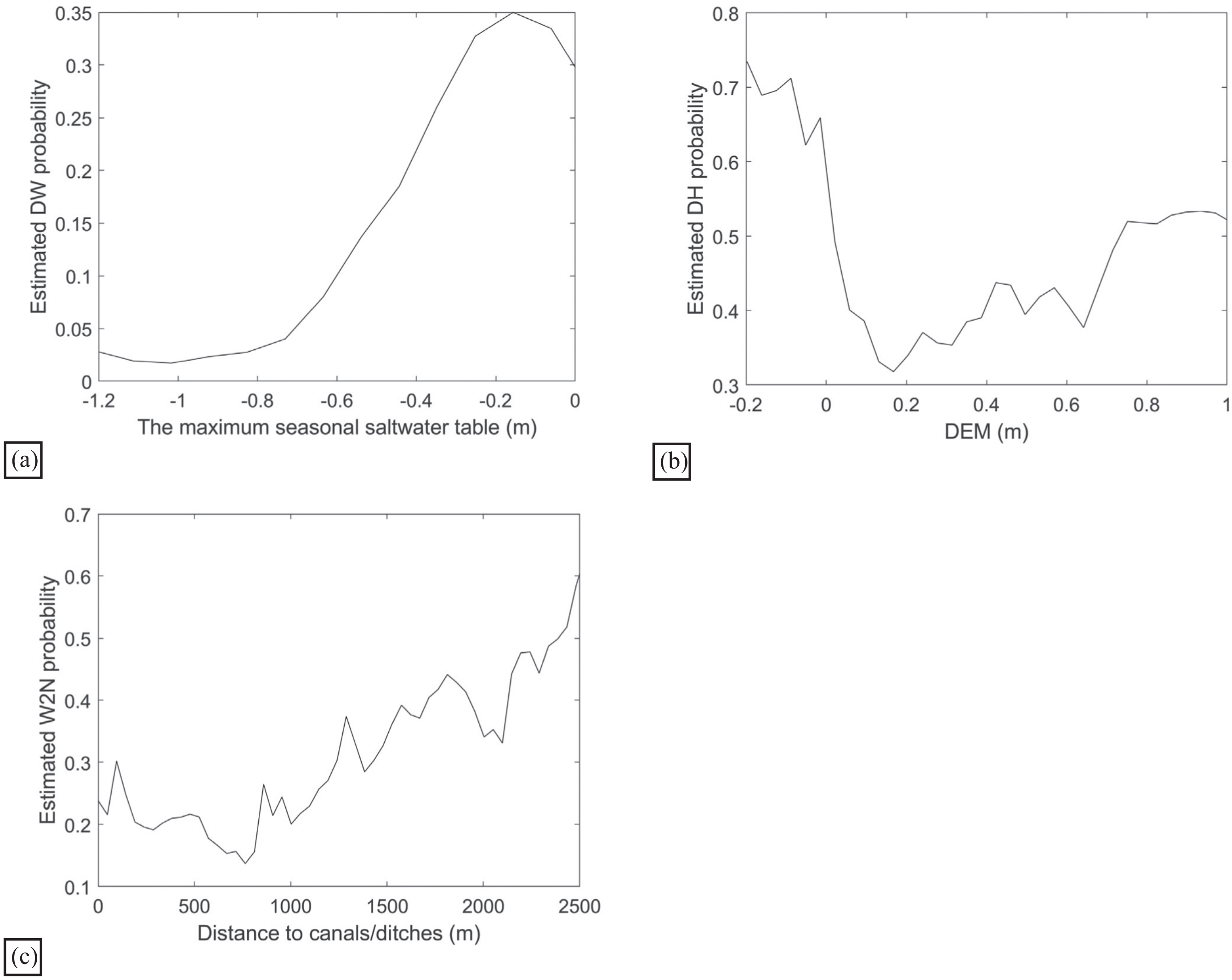

Fig. 5. Partial dependence plot (PDP) of the key driver for (a) DW and NDW, (b) DH and NDH, and (c) W2N and W2H. X-axes are SWT_{max} (unit: m) in (a), DEM (unit: m) in (b), and distance to canals/ditches (unit: m) in (c), and y-axes are estimated (a) DW, (b) DH, and (c) W2N probability, respectively.

(corresponding to DEM = 0 m, Fig. 5b) and 0.32 m below the land surface (corresponding to DEM = 0.7 m, Fig. 5b) were critical upper and lower bounds of GWT_{max} for the maintenance of emergent herbaceous wetlands, respectively. Once GWT_{max} is beyond this range, emergent herbaceous wetland downgrading is more likely to occur.

Fig. 4a suggests that SWT_{max} largely affected woody wetland downgrading, however, the key factor in determining the fate of the downgraded woody wetlands (W2N versus W2H) is their distances to canals/ditches (Fig. 4c). Fig. 5c shows that downgraded woody wetlands were more likely to convert to emergent herbaceous wetlands (W2H) if they were within 1000 m of canals/ditches. When the downgraded woody wetlands were far away from the canals/ditches, i.e., > 1000 m from the canals/ditches, they tended to disappear (W2N).

Among the five predictors, PIT was the least important variable in the three RF models (Fig. 4). To understand the PIT's impacts on wetland downgrading, we plotted the PDP of PIT for all three wetland downgrading cases (Fig. 7). Fig. 7a and b show that the PDP reached its maximum when PIT ≈ 1 (inundation sustained year-round) or PIT ≈ 0 (the groundwater level was never above the land surface during the analysis period). This finding suggests that wetland downgrading happened only during extremely prolonged inundations (PIT ≈ 1) or during periods when the groundwater level never rises to the land surface (PIT ≈ 0). In the study area, we found that these extreme conditions accounted for only about 12.7 % (RF1) and 12.0 % (RF2) of cases during 1995–2019. In RF3, the estimated W2N probability did not change with PIT, but fluctuated around 0.32 (Fig. 7c). These may partially explain why PIT was less important than the other four predictors in the RF classification models.

4. Discussion

4.1. Driving hydrogeomorphic factors of coastal wetland downgrading

Consistent with previous studies (Conner et al., 2002; Day et al., 2008; He et al., 2022; Rodríguez-Iturbe and Porporato, 2007; Smart et al., 2020; Stagg et al., 2020; Ury et al., 2021; Williams et al., 2003; Winter, 2000; Zhang et al., 2018, 2019), this study found that disruption of hydrogeomorphic processes can lead to coastal wetland downgrading. Furthermore, we found that for different types of wetland downgrading, the most important hydrogeomorphic variable varies: SWT_{max} is found to be the most paramount variable for coastal woody wetland downgrading; emergent herbaceous wetlands were susceptible to floods and droughts; and distances to canals played a dominant role in determining the fates of downgraded woody wetlands (Fig. 4).

4.1.1. Woody wetlands most susceptible to saltwater intrusion

Our results support previous research that coastal marshes are considered salt-tolerant while woody wetlands are salt-sensitive (Kirwan and Gedan, 2019; Kirwan et al., 2007; Schieder et al., 2018). Rising saltwater

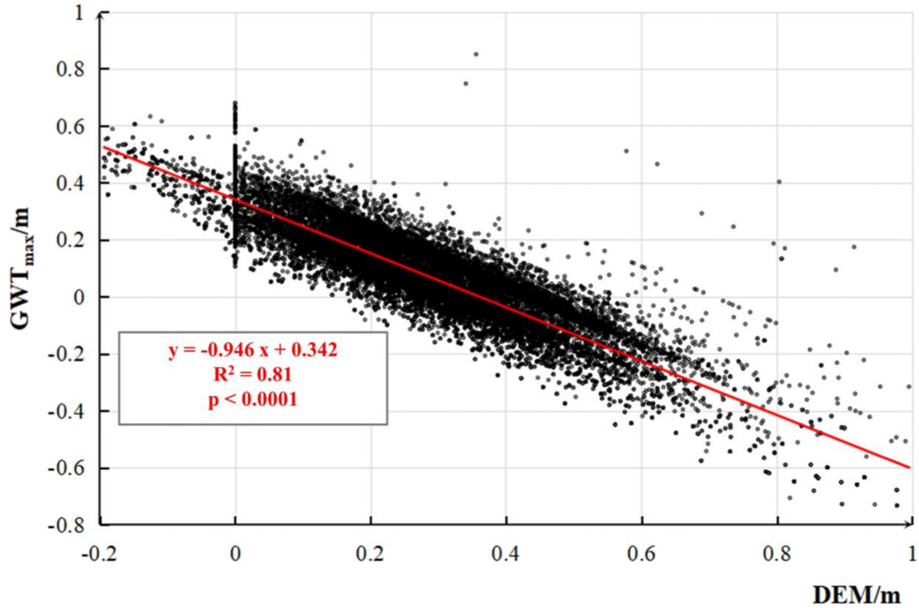

Fig. 6. The relationship between GWT_{max} (y-axis, unit: m) and DEM (x-axis, unit: m) in emergent herbaceous wetlands. The red line represents the fitted linear regression for GWT_{max} against DEM ($R^2 = 0.81$, $p < 0.0001$).

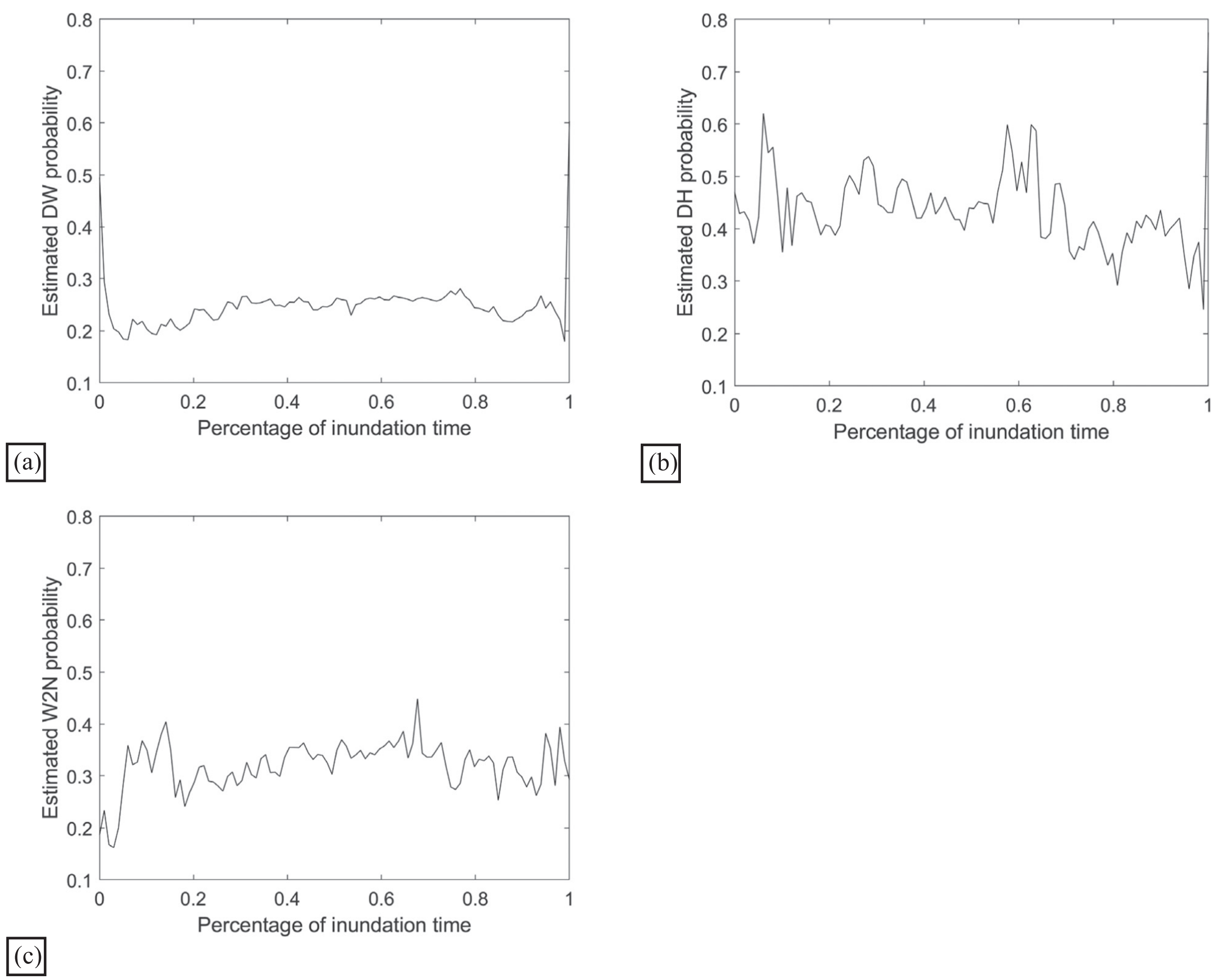

Fig. 7. Partial dependence plot of the variable PIT for (a) DW and NDW, (b) DH and NDH, and (c) W2N and W2H.

tables can negatively impact woody wetlands by altering the soil conditions (Conner et al., 1997). As saltwater rises, it can penetrate the soil and lead to salt accumulation, which can be toxic to many tree species (Pezeshki et al., 1990; Van Mensvoort et al., 1985). This results in the replacement of native freshwater-dependent woody vegetation with salt-tolerant marshes (i.e., woody wetlands downgrading to emergent herbaceous wetlands), in extreme cases, complete conversion of the wetland to non-vegetated areas (woody wetland loss).

4.1.2. Emergent herbaceous wetlands most vulnerable to drought and inundation

For emergent herbaceous wetlands, droughts and floods are more critical. When the area experiences below-normal precipitation, meteorological drought occurs. Drought can increase chronic stress through reduced water availability and elevated salinity levels, thereby adversely impacting the coastal wetland ecosystems, especially the coastal marshes with higher DEM (Hughes et al., 2012; Rodríguez-Iturbe and Porporato, 2007; Silliman et al., 2005; Zheng et al., 2022). If the drought lasts longer and/or becomes severe, it finally leads to the dieback of the emergent herbaceous wetland (Wetzel and Kitchens, 2007). On the other hand, excessive heavy rainfall-induced flooding often gives rise to inundations. High water tables from flooding can impact soil oxygen availability for root aerobic respiration and vegetation growth (Fagherazzi et al., 2019; Zhang et al., 2019), contributing to the fragmentation and loss of coastal herbaceous wetlands (Stagg et al., 2020).

4.1.3. Distances to canals key to the fates of downgraded woody wetlands

Variable importance analysis in RF models shows that the distance between the wetlands and the canals/ditches was the key factor that determines the final fates of downgraded woody wetlands (W2N versus W2H, Fig. 4c). Artificial canals and ditches were initially constructed to drain the wetlands by lowering groundwater for agriculture and forestry from the 1960s through the 1980s (Poulter, 2005; Ury et al., 2021). Because the impact of drainage canals and ditches on groundwater decreases as the distance increases (Liu et al., 2017), the resulting groundwater table (GWT) becomes funnel-shaped (Nuruddin and Leng, 2002; Vissers et al., 1999), i.e., GWT is deeper (shallower) in the areas close to (far from) the canal/ditch. During the flooding years/seasons, canals/ditches can effectively drain the water and avoid prolonged inundation. While during drought periods, the low elevation of canals/ditches makes them easier to obtain and retain water. As a result, emergent herbaceous plants are more likely to survive in the areas near the canals/ditches compared to those in the areas far away from canals/ditches where droughts and floods are more likely to occur when precipitation fluctuates. This finding also implied that, although artificial drainage networks were widely considered to serve as conduits for saltwater to move further inland (Bhattachan et al., 2018; Smart et al., 2020; Ury et al., 2021), the salinity level near the canals/ditches in our study area may be still within the tolerance of marshes; thus, they can survive near canals/ditches. Obviously, for downgraded woody wetland ecosystems, W2H is better than W2N as emergent herbaceous wetlands can provide more ecological services than non-vegetated areas (Zhang et al., 2021b). In addition, results indicated that the impacts of canals/ditches on woody and emergent herbaceous wetland downgrading were minimal (Fig. 4a and b). However, Li et al. (2012) found that the drainage ditches speed up the wetland downgrading in Zoige Plateau. The divergence impacts of canals/ditches on wetland downgrading may be related to the characteristics of canals/ditches (e.g., width, depth, whether connected to the saltwater) and need further detailed investigations.

4.1.4. Other potential driving hydrogeomorphic factors

This study investigated five potential hydrogeomorphic variables (elevations (DEM), distance to canals/ditches, the maximum seasonal saltwater table (SWT_{max}), the maximum seasonal groundwater table (GWT_{max}), and the percentage of inundation time (PIT)) of coastal wetland downgrading. Some other hydrological variables, such as soil water content, precipitation, and evapotranspiration, may also contribute to wetland downgrading (Hu et al., 2020; Li et al., 2020; Melly et al., 2017; Meng et al., 2017; Zhang et al., 2018). However, the inclusion of these variables did not improve the performance of fitted RF models substantially, and their relative importance was close to zero (not shown). It is not surprising as soil water content, precipitation, and evapotranspiration are all highly correlated to the variations of DEM, GWT_{max}, and SWT_{max}. Thus, adding more correlated variables (e.g., autocorrelation) could not further provide more information to improve the RF models' classification performances. These results also highlight the importance of DEM, GWT_{max}, and SWT_{max} to wetland downgrading.

4.2. Implications for coastal wetland downgrading predictions and conservation planning

Saltwater intrusion induced by climate change and sea-level rise (SLR) is often seen as an "invisible" threat to coastal wetlands (Smart et al., 2020; Tully et al., 2019). The lack of extensive and long-term monitoring of groundwater and saltwater tables prevents us from understanding and predicting wetland resilience in a warming climate. Our analysis suggests that machine learning models combined with remote sensing and hydrological modeling provide a promising way to monitor and predict the dynamics of wetlands under climate change, SLR, and anthropogenic activities. In this study, we trained RF models with remote sensing data and simulated hydrological variables from a process-based hydrological model, PIHM-Wetland, to understand how changes in hydrogeomorphic processes contribute to coastal wetland downgrading. We identified different dominant drivers affecting coastal wetland downgrading and quantified their critical thresholds among different types of wetlands. These results are crucial for stakeholders and wetland managers to plan and implement more targeted and efficient adaptation and restoration measures for different types of wetlands as the Intergovernmental Panel on Climate Change (IPCC, 2021) projects sea level will increase faster in the future with the east USA coast as a hotspot (Oppenheimer et al., 2019; Sweet et al., 2022). Although all the findings in this study are ARNWR-specific, the machine learning-hydrological model coupled method used here is highly transferable. It can be applied to other regional coastal wetland ecosystems as long as the climate-forcing data required for driving the hydrological model are available.

4.3. Limitations

We acknowledge that there are some levels of uncertainties in the detected locations and timing of wetland downgrading. A detailed discussion of this can be found in He et al. (2022). In addition, some uncertainties exist in simply using the static digital elevation model (DEM) for the study period (1995–2019). The geomorphologic change of coastal marshes may have some impacts on seawater propagation, thereby affecting coastal freshwater-saltwater interaction (Zhang et al., 2022b). The RF models used in this study are exemplary for investigating the combined effects and relative importance of hydrogeomorphic variables impacting coastal wetland downgrading, although the models cannot illustrate the detailed physiological processes behind the downgrading processes. Despite these limitations, results from the machine learning-hydrological model coupled method provide insights into the relative importance of different hydrogeomorphic processes in different types of wetland downgrading and the critical thresholds of dominant hydrogeomorphic factors, which could facilitate more accurate physical model-based and regional-scale assessments of coastal wetland downgrading. Furthermore, this study acts as an essential baseline for future prediction of the probability of wetland downgrading. The knowledge learned from this study can benefit policymakers, landowners, and wetland managers in better foreseeing the interventions and adaptation efforts that will be required in the immediate and/or far future.

5. Conclusions

Our study provides a comprehensive analysis of the combined impacts and the relative importance of various driving hydrogeomorphic factors, including elevations (DEM), distance to canals/ditches, the maximum seasonal saltwater and groundwater table (SWT_{max} and GWT_{max}), and the percentage of inundation time (PIT), in explaining spatial-temporal variations of wetland downgrading by using random forest classification models. We fitted three random forest classifiers for three types of coastal wetland downgrading detected in the southeast part of the Alligator River National Wildlife Refuge in Dare County, North Carolina, USA: woody wetland loss, emergent herbaceous wetland loss, and woody wetlands downgrading to emergent herbaceous wetlands. High overall accuracies (> 0.97) and kappa coefficients (> 0.94) and low errors of omission and commission (< 0.05) indicated that these random forest models could well distinguish downgraded wetlands from non-downgraded wetlands and accurately classify woody wetlands downgrading to non-vegetated areas from downgrading to emergent herbaceous wetlands.

Random forest model results demonstrated that multiple hydrogeomorphic variables collectively resulted in coastal wetland downgrading while the dominant driver affecting the downgrading varied among different types of wetlands. Woody wetlands were susceptible to saltwater intrusion. The partial dependence plot revealed a sigmoidal response of woody wetland downgrading probability to SWT_{max}, with SWT_{max} below the land surface by 0.2–0.8 m critical to woody wetlands. When SWT_{max} is above 0.8 m below the surface, a miniature rise of SWT_{max} would cause a considerable increase in the probability of woody wetland downgrading. Unlike woody wetlands, emergent herbaceous wetlands were vulnerable to inundation (low elevations) and droughts (high elevations). GWT_{max} within the range of 0.34 m above the land surface and 0.32 m below the land surface might be suitable for the maintenance of emergent herbaceous wetlands. For downgraded woody wetlands, their distances to canals/ditches played a crucial role in determining their fates after downgrading. The downgraded woody wetlands were more likely to disappear if they were > 1000 m away from canals/ditches. However, for those close to canals/ditches (within 1000 m of canals/ditches), although they also downgraded, they were still wetlands (emergent herbaceous wetlands) and could keep providing wetland-specific services.

This study comprehensively analyzed the driving factors of wetland downgrading from a hydrogeomorphic aspect by combining machine learning models and hydrological modeling. The machine learning-hydrological model coupled method used in this study presents an encouraging way toward better regional understanding and predictions of wetland downgrading. The results of this study shed light on the importance of various and targeted management and/or restoration activities for different types of wetlands.

CRediT authorship contribution statement

Keqi He: Conceptualization, Methodology, Data curation, Software, Validation, Formal analysis, Investigation, Resources, Writing – original draft, Writing – review & editing, Visualization. **Wenhong Li:** Conceptualization, Methodology, Resources, Writing – review & editing, Supervision, Project administration, Funding acquisition. **Yu Zhang:** Software, Data curation, Writing – review & editing. **Ge Sun:** Writing – review & editing. **Steve G. McNulty:** Writing – review & editing. **Neal E. Flanagan:** Writing – review & editing. **Curtis J. Richardson:** Writing – review & editing.

Data availability

Data and codes can be accessed in GitHub via https://github.com/hkqcqq/Wtldegrad_RF.git.

Declaration of competing interest

The authors declare that they have no known competing financial interests or personal relationships that could have appeared to influence the work reported in this paper.

Acknowledgment

This work was supported by Duke Nicholas School Dean's Research Fund.

Appendix A. Supplenmentary data

References

Abbasian, H., Solgi, E., Hosseini, S.M., Kia, S.H., 2022. Modeling terrestrial net ecosystem exchange using machine learning techniques based on flux tower measurements. Ecol. Model. 466, 109901. https://doi.org/10.1016/j.ecolmodel.2022.109901.
Ackoff, R.L., 1994. It's a mistake! Syst. Practice 7 (1), 3–7. https://doi.org/10.1007/BF02169161.
Aguilos, M., Warr, I., Irving, M., Gregg, O., Grady, S., Peele, T., Noormets, A., Sun, G., Liu, N., McNulty, S., Pettay, F., 2022. The unabated atmospheric carbon losses in a drowning wetland Forest of North Carolina: a point of no return? Forests. 13 (8), 1264. https://doi.org/10.3390/f13081264.
ArcGIS, 2016. Version 10.5.1. Environmental Systems Research Institute, Inc, Redlands, CA.
Bayley, S., Falessi, D., 2018. Optimizing Prediction Intervals by Tuning Random Forest Via Meta-validation. arXiv Preprint arXiv:1801.07194. https://doi.org/10.48550/arXiv.1801.07194.
Belmokre, A., Mihoubi, M.K., Santillán, D., 2019. Analysis of dam behavior by statistical models: application of the random forest approach. KSCE J. Civ. Eng. 23 (11), 4800–4811. https://doi.org/10.1007/s12205-019-0339-0.
Bhattachan, A., Emanuel, R.E., Ardon, M., Bernhardt, E.S., Anderson, S.M., Stillwagon, M.G., Ury, E.A., BenDor, T.K., Wright, J.P., 2018. Evaluating the effects of land-use change and future climate change on vulnerability of coastal landscapes to saltwater intrusion. Elem. Sci. Anth. 6. https://doi.org/10.1525/elementa.316.
Blankespoor, B., Dasgupta, S., Laplante, B., 2014. Sea-level rise and coastal wetlands. Ambio. 43 (8), 996–1005. https://doi.org/10.1007/s13280-014-0500-4.
Breiman, L., 2001. Random forests. Mach. Learn. 45 (1), 5–32. https://doi.org/10.1023/A:1010933404324.
Carranza, C., Nolet, C., Pezij, M., Van Der Ploeg, M., 2021. Root zone soil moisture estimation with Random Forest. J. Hydrol. 593, 125840. https://doi.org/10.1016/j.jhydrol.2020.125840.
Church, J.A., White, N.J., 2011. Sea-level rise from the late 19th to the early 21st century. Surv. Geophys. 32 (4), 585–602. https://doi.org/10.1007/s10712-011-9119-1.
Cloern, J.E., Abreu, P.C., Carstensen, J., Chauvaud, L., Elmgren, R., Grall, J., Greening, H., Johansson, J.O., Kahru, M., Sherwood, E.T., Xu, J., 2016. Human activities and climate variability drive fast-paced change across the world's estuarine–coastal ecosystems. Glob. Chang. Biol. 22 (2), 513–529. https://doi.org/10.1111/gcb.13059.
Cohen, J., 1960. A coefficient of agreement for nominal scales. Educ. Psychol. Meas. 20 (1), 37–46. https://doi.org/10.1177/001316446002000104.
Conner, W.H., McLeod, K.W., McCarron, J.K., 1997. Flooding and salinity effects on growth and survival of four common forested wetland species. Wetl. Ecol. Manag. 5, 99–109. https://doi.org/10.1023/A:1008251127131.
Conner, W.H., Mihalia, I., Wolfe, J., 2002. Tree community structure and changes from 1987 to 1999 in three Louisiana and three South Carolina forested wetlands. Wetlands. 22 (1), 58–70. https://doi.org/10.1672/0277-5212(2002)022[0058:TCSACF]2.0.CO;2.
Cui, L., Gao, C., Zhou, D., Mu, L., 2014. Quantitative analysis of the driving forces causing declines in marsh wetland landscapes in the Honghe region, northeast China, from 1975 to 2006. Environ. Earth Sci. 71 (3), 1357–1367. https://doi.org/10.1007/s12665-013-2542-5.
Cutler, D.R., Edwards Jr., T.C., Beard, K.H., Cutler, A., Hess, K.T., Gibson, J., Lawler, J.J., 2007. Random forests for classification in ecology. Ecology. 88 (11), 2783–2792. https://doi.org/10.1890/07-0539.1.
Dangendorf, S., Marcos, M., Wöppelmann, G., Conrad, C.P., Frederikse, T., Riva, R., 2017. Reassessment of 20th century global mean sea level rise. Proc. Natl. Acad. Sci. U. S. A. 114 (23), 5946–5951. https://doi.org/10.1073/pnas.1616007114.
Danielson, J.J., Poppenga, S.K., Brock, J.C., Evans, G.A., Tyler, D.J., Gesch, D.B., Thatcher, C.A., Barras, J.A., 2016. Topobathymetric elevation model development using a new methodology-Coastal National Elevation Database. J. Coast. Res. SI 76, 75–89. https://doi.org/10.2112/SI76-008.
Danielson, J.J., Poppenga, S.K., Tyler, D.J., Palaseanu-Lovejoy, M., Gesch, D.B., 2018. Coastal National Elevation Database: U.S. Geological Survey Fact Sheet 2018–3037. https://doi.org/10.3133/2018 (2 pp.).
Day, J.W., Christian, R.R., Boesch, D.M., Yáñez-Arancibia, A., Morris, J., Twilley, R.R., Naylor, L., Schaffner, L., 2008. Consequences of climate change on the ecogeomorphology of coastal wetlands. Estuar. Coasts 31 (3), 477–491. https://doi.org/10.1007/s12237-008-9047-6.
Dewitz, J., 2021. National Land Cover Database (NLCD) 2019 Products (ver. 2.0, June 2021) [Dataset]. US Geological Survey: Sioux Falls, SD, USA. https://doi.org/10.5066/P9KZCM54.
Ellison, J.C., 1999. Impacts of sediment burial on mangroves. Mar. Pollut. Bull. 37 (8), 420–426. https://doi.org/10.1016/S0025-326X(98)00122-2.
Fagherazzi, S., Anisfeld, S.C., Blum, L.K., Long, E.V., Feagin, R.A., Fernandes, A., Kearney, W.S., Williams, K., 2019. Sea level rise and the dynamics of the marsh-upland boundary. Front. Environ. Sci. 7, 25. https://doi.org/10.3389/fenvs.2019.00025.
Feng, F., Li, K.C., Shen, J., Zhou, Q., Yang, X., 2020. Using cost-sensitive learning and feature selection algorithms to improve the performance of imbalanced classification. IEEE Access 8, 69979–69996. https://doi.org/10.1109/ACCESS.2020.2987364.
Flanagan, N.E., Richardson, C.J., 2010. A multi-scale approach to prioritize wetland restoration for watershed-level water quality improvement. Wetl. Ecol. Manag. 18, 695–706. https://doi.org/10.1007/s11273-010-9188-9.
Friedman, J., 2001. Greedy function approximation: a gradient boosting machine. Ann. Stat. 29 (5), 1189–1232. https://doi.org/10.1214/aos/1013203451.
Gao, X.H., 2018. Memberships, distance and proper-motion of the open cluster NGC 188 based on a machine learning method. Astrophys. Space Sci. 363 (11), 1–8. https://doi.org/10.1007/s10509-018-3453-4.

Gray, P.C., Chamorro, D.F., Ridge, J.T., Kerner, H.R., Ury, E.A., Johnston, D.W., 2021. Temporally generalizable land cover classification: a recurrent convolutional neural network unveils major coastal change through time. Remote Sens. 13 (19), 3953. https://doi.org/10.3390/rs13193953.

Grenfell, M.C., Ellery, W.N., Garden, S.E., Dini, J., Van der Valk, A.G., 2007. The language of intervention: a review of concepts and terminology in wetland ecosystem repair. Water SA 33, 43–50. https://doi.org/10.4314/wsa.v33i1.47870.

Gupta, A.D., 1985. Approximation of salt-water interface fluctuation in an unconfined coastal aquifer. Ground Water 23 (6), 783–794. https://doi.org/10.1111/j.1745-6584.1985.tb01958.x.

Hackney, C.T., Yelverton, G.F., 1990. Effects of human activities and sea level rise on wetland ecosystems in the Cape Fear River Estuary, North Carolina, USA. Wetland Ecology and Management: Case Studies. Springer, Dordrecht, pp. 55–61 https://doi.org/10.1007/978-94-009-2115-3_7.

Hastie, T.J., Tibshirani, R.J., Friedman, J.H., 2001. The Elements of Statistical Learning: Data Mining, Inference, and Prediction. Springer, New York, USA.

He, Q., Silliman, B.R., 2019. Climate change, human impacts, and coastal ecosystems in the Anthropocene. Curr. Biol. 29 (19), R1021–R1035. https://doi.org/10.1016/j.cub.2019.08.042.

He, K., Zhang, Y., Li, W., Sun, G., McNulty, S., 2022. Detecting coastal wetland degradation by combining remote sensing and hydrologic modeling. Forests. 13 (3), 411. https://doi.org/10.3390/f13030411.

Hikouei, I.S., Christian, J., Kim, S.S., Sutter, L.A., Durham, S.A., Yang, J.J., Vickery, C.G., 2021. Use of Random Forest model to identify the relationships among vegetative species, salt marsh soil properties, and interstitial water along the Atlantic Coast of Georgia. Infrastructures. 6 (5), 70. https://doi.org/10.3390/infrastructures6050070.

Hu, T., Liu, J., Zheng, G., Zhang, D., Huang, K., 2020. Evaluation of historical and future wetland degradation using remote sensing imagery and land use modeling. Land Degrad. Dev. 31 (1), 65–80. https://doi.org/10.1002/ldr.3429.

Huang, Y., Ciais, P., Luo, Y., Zhu, D., Wang, Y., Qiu, C., Goll, D.S., Guenet, B., Makowski, D., De Graaf, I., Leifeld, J., 2021. Tradeoff of CO2 and CH4 emissions from global peatlands under water-table drawdown. Nat. Clim. Chang. 11 (7), 618–622. https://doi.org/10.1038/s41558-021-01059-w.

Hughes, A.L., Wilson, A.M., Morris, J.T., 2012. Hydrologic variability in a salt marsh: assessing the links between drought and acute marsh dieback. Estuar. Coast. Shelf Sci. 111, 95–106. https://doi.org/10.1016/j.ecss.2012.06.016.

IPCC, 2021. Climate change 2021: the physical science basis. In: Stocker, T.F., Qin, D., Plattner, G.-K., Tignor, M., Allen, S.K., Boschung, J., Nauels, A., Xia, Y., Bex, V., Midgley, P.M. (Eds.), Contribution of Working Group I to the Keeley Assessment Report of the Intergovernmental Panel on Climate Change. Cambridge University Press, Cambridge, United Kingdom and New York, NY, USA, p. 1535.

Irwin, J.R., Danielson, J.J., Robbins, T.J., 2021. Coastal Carolinas Topobathymetric Model: Field Validation Data, 2021. Geological Survey data release, U.S https://doi.org/10.5066/P902W30G.

Kemp, A.C., Horton, B.P., Culver, S.J., 2009. Distribution of modern salt-marsh foraminifera in the Albemarle–Pamlico estuarine system of North Carolina, USA: implications for sea-level research. Mar. Micropaleontol. 72 (3–4), 222–238. https://doi.org/10.1016/j.marmicro.2009.06.002.

Kesikoglu, M.H., Atasever, U.H., Dadaser-Celik, F., Ozkan, C., 2019. Performance of ANN, SVM and MLH techniques for land use/cover change detection at Sultan Marshes wetland, Turkey. Water Sci. Technol. 80 (3), 466–477. https://doi.org/10.2166/wst.2019.290.

Kirwan, M.L., Gedan, K.B., 2019. Sea-level driven land conversion and the formation of ghost forests. Nat. Clim. Chang. 9 (6), 450–457. https://doi.org/10.1038/s41558-019-0488-7.

Kirwan, M.L., Megonigal, J.P., 2013. Tidal wetland stability in the face of human impacts and sea-level rise. Nature. 504 (7478), 53–60. https://doi.org/10.1038/nature12856.

Kirwan, M.L., Kirwan, J.L., Copenheaver, C.A., 2007. Dynamics of an estuarine forest and its response to rising sea level. J. Coast. Res. 232, 457–463. https://doi.org/10.2112/04-0211.1.

Li, M., Li, L., Liao, H., Huang, Z., Huang, W., 2012. The influence of drainage on wetland degradation in Zoige plateau. Disaster Adv. 5 (4), 659–666.

Li, Z., Gao, P., Hu, X., Yi, Y., Pan, B., You, Y., 2020. Coupled impact of decadal precipitation and evapotranspiration on peatland degradation in the Zoige basin, China. Phys. Geogr. 41 (2), 145–168. https://doi.org/10.1080/02723646.2019.1620579.

Liu, Q., Mou, X., Cui, B., Ping, F., 2017. Regulation of drainage canals on the groundwater level in a typical coastal wetlands. J. Hydrol. 555, 463–478. https://doi.org/10.1016/j.jhydrol.2017.10.035.

Long, A.L., Kettenring, K.M., Hawkins, C.P., Neale, C.M., 2017. Distribution and drivers of a widespread, invasive wetland grass, Phragmites australis, in wetlands of the Great Salt Lake, Utah, USA. Wetlands 37 (1), 45–57. https://doi.org/10.1007/s13157-016-0838-4.

Masson-Delmotte, V., Zhai, P., Pirani, A., Connors, S.L., Péan, C., Berger, S., Caud, N., Chen, Y., Goldfarb, L., Gomis, M.I., Huang, M., Leitzell, K., Lonnoy, E., Matthews, J.B.R., Maycock, T.K., Waterfield, T., Yelekçi, O., Yu, R., Zhou, B. (Eds.), 2021. Climate Change 2021: The Physical Science Basis. Contribution of Working Group I to the Sixth Assessment Report of the Intergovernmental Panel on Climate Change. Cambridge University Press, Cambridge, United Kingdom and New York, NY, USA (In press).

Maxwell, A.E., Warner, T.A., Strager, M.P., 2016. Predicting palustrine wetland probability using random forest machine learning and digital elevation data-derived terrain variables. Photogramm. Eng. Remote. Sens. 82 (6), 437–447. https://doi.org/10.14358/PERS.82.6.437.

Mcleod, E., Chmura, G.L., Bouillon, S., Salm, R., Björk, M., Duarte, C.M., Lovelock, C.E., Schlesinger, W.H., Silliman, B.R., 2011. A blueprint for blue carbon: toward an improved understanding of the role of vegetated coastal habitats in sequestering CO2. Front. Ecol. Environ. 9 (10), 552–560. https://doi.org/10.1890/110004.

Melly, B.L., Schael, D.M., Gama, P.T., 2017. Perched wetlands: an explanation to wetland formation in semi-arid areas. J. Arid Environ. 141, 34–39. https://doi.org/10.1016/j.jaridenv.2017.02.004.

Meng, W., He, M., Hu, B., Mo, X., Li, H., Liu, B., Wang, Z., 2017. Status of wetlands in China: a review of extent, degradation, issues and recommendations for improvement. Ocean Coast. Manag. 146, 50–59. https://doi.org/10.1016/j.ocecoaman.2017.06.003.

Millennium ecosystem assessment, M.E.A, 2005. Ecosystems and Human Well-being. vol. 5. Island press, Washington, DC.

Mitsch, W.J., Gosselink, J.G., 2015. Wetlands. 5th ed. John Wiley, Inc., New York, NY, USA.

Mohammed, R., Rawashdeh, J., Abdullah, M., 2020. Machine learning with oversampling and undersampling techniques: overview study and experimental results. IEEE 2020 11th International Conference on Information and Communication Systems (ICICS), Irbid, Jordan, Apr 7-9, 2020, pp. 243–248 https://doi.org/10.1109/ICICS49469.2020.239556.

Moon, J., Kim, Y., Son, M., Hwang, E., 2018. Hybrid short-term load forecasting scheme using random forest and multilayer perceptron. Energies. 11 (12), 3283. https://doi.org/10.3390/en11123283.

Moorhead, K.K., Brinson, M.M., 1995. Response of wetlands to rising sea level in the lower coastal plain of North Carolina. Ecol. Appl. 5 (1), 261–271. https://doi.org/10.2307/1942068.

Moorhead, K.K., Cook, A.E., 1992. A comparison of hydric soils, wetlands, and land use in coastal North Carolina. Wetlands. 12 (2), 99–105. https://doi.org/10.1007/BF03160591.

Morton, R.A., Barras, J.A., 2011. Hurricane impacts on coastal wetlands: a half-century record of storm-generated features from southern Louisiana. J. Coast. Res. 27 (6A), 27–43. https://doi.org/10.2112/JCOASTRES-D-10-00185.1.

Mutanga, O., Adam, E., Cho, M.A., 2012. High density biomass estimation for wetland vegetation using WorldView-2 imagery and random forest regression algorithm. Int. J. Appl. Earth Obs. Geoinf. 18, 399–406. https://doi.org/10.1016/j.jag.2012.03.012.

Nuruddin, A.A., Leng, H., 2002. Monitoring Peat Water Level as an Early Warning Indicator for Peat Forest Fire Management Programme. Prevention and Control Of Fire in Peatlands. 57.

Oppenheimer, M., Glavovic, B.C., Hinkel, J., van de Wal, R., Magnan, A.K., Abd-Elgawad, A., Cai, R., Cifuentes-Jara, M., DeConto, R.M., Ghosh, T., Hay, J., Isla, F., Marzeion, B., Meyssignac, B., Sebesvari, Z., 2019. Sea level rise and implications for low-lying islands, coasts and communities. In: Pörtner, H.-O., Roberts, D.C., Masson-Delmotte, V., Zhai, P., Tignor, M., Poloczanska, E., Mintenbeck, K., Alegría, A., Nicolai, M., Okem, A., Petzold, J., Rama, B., Weyer, N.M. (Eds.), IPCC Special Report on the Ocean and Cryosphere in a Changing Climate. Cambridge University Press, Cambridge, UK and New York, NY, USA, pp. 321–445 https://doi.org/10.1017/9781009157964.006.

Pawluszek-Filipiak, K., Borkowski, A., 2020. On the importance of train–test split ratio of datasets in automatic landslide detection by supervised classification. Remote Sens. 12 (18), 3054. https://doi.org/10.3390/rs12183054.

Peltola, O., Vesala, T., Gao, Y., Räty, O., Alekseychik, P., Aurela, M., Chojnicki, B., Desai, A.R., Dolman, A.J., Euskirchen, E.S., Friborg, T., 2019. Monthly gridded data product of northern wetland methane emissions based on upscaling eddy covariance observations. Earth Syst. Sci. Data. 11 (3), 1263–1289. https://doi.org/10.5194/essd-11-1263-2019.

Peng, K., Jiang, W., Deng, Y., Liu, Y., Wu, Z., Chen, Z., 2020. Simulating wetland changes under different scenarios based on integrating the random forest and CLUE-S models: a case study of Wuhan Urban Agglomeration. Ecol. Indic. 117, 106671. https://doi.org/10.1016/j.ecolind.2020.106671.

Perry, G.L., Dickson, M.E., 2018. Using machine learning to predict geomorphic disturbance: the effects of sample size, sample prevalence, and sampling strategy. J. Geophys. Res. Earth Surf. 123 (11), 2954–2970. https://doi.org/10.1029/2018JF004640.

Pezeshki, S.R., DeLaune, R.D., Patrick Jr., W.H., 1990. Flooding and saltwater intrusion: potential effects on survival and productivity of wetland forests along the US Gulf Coast. For. Ecol. Manag. 33, 287–301. https://doi.org/10.1016/0378-1127(90)90199-L.

Polo, J.F., Ramis, F.J.R., 1983. Simulation of salt water–fresh water interface motion. Water Resour. Res. 19 (1), 61–68. https://doi.org/10.1029/WR019i001p00061.

Poulter, B., 2005. Interactions between Landscape Disturbance and Gradual Environmental Change: Plant Community Migration in Response to Fire and Sea Level Rise. Duke University.

Raj, D., Khamis, S.H., 1958. Some remarks on sampling with replacement. Ann. Math. Stat. 550-7. https://doi.org/10.1214/aoms/1177706630.

Richardson, C.J., 2012. Pocosins: evergreen shrub bogs of the southeast. Chapter 14 (pp. 189-202). In: Batzer, D.P., Baldwin, A.H. (Eds.), Wetland Habitats of North America: Ecology and Conservation Concerns. University of California Press, Berkeley.

Robinson, O.J., Ruiz-Gutierrez, V., Fink, D., 2018. Correcting for bias in distribution modelling for rare species using citizen science data. Divers. Distrib. 24 (4), 460–472. https://doi.org/10.1111/ddi.12698.

Rodríguez-Iturbe, I., Porporato, A., 2007. Ecohydrology of Water-controlled Ecosystems: Soil Moisture and Plant Dynamics. Cambridge University Press, New York https://doi.org/10.1017/CBO9780511535727.

Rohmer, J., Idier, D., Paris, F., Pedreros, R., Louisor, J., 2018. Casting light on forcing and breaching scenarios that lead to marine inundation: combining numerical simulations with a random-forest classification approach. Environ. Model. Softw. 104, 64–80. https://doi.org/10.1016/j.envsoft.2018.03.003.

Sallenger, A.H., Doran, K.S., Howd, P.A., 2012. Hotspot of accelerated sea level rise on the Atlantic coast of North America. Nat. Clim. Chang. 2, 884–888. https://doi.org/10.1038/nclimate1597.

Santoso, H., Tani, H., Wang, X., 2017. Random Forest classification model of basal stem rot disease caused by Ganoderma boninense in oil palm plantations. Int. J. Remote Sens. 38 (16), 4683–4699. https://doi.org/10.1080/01431161.2017.1331474.

Schieder, N.W., Walters, D.C., Kirwan, M.L., 2018. Massive upland to wetland conversion compensated for historical marsh loss in Chesapeake Bay, USA. Estuar. Coasts 41 (4), 940–951. https://doi.org/10.1007/s12237-017-0336-9.

Schuerch, M., Spencer, T., Temmerman, S., Kirwan, M.L., Wolff, C., Lincke, D., McOwen, C.J., Pickering, M.D., Reef, R., Vafeidis, A.T., Hinkel, J., 2018. Future response of global coastal wetlands to sea-level rise. Nature. 561 (7722), 231–234. https://doi.org/10.1038/s41586-018-0476-5.

Senter, J., 2003. Live dunes and ghost forests: stability and change in the history of North Carolina's maritime forests. N. C. Hist. Rev. 80 (3), 334–371.
Shamir, U., Dagan, G., 1971. Motion of the seawater interface in coastal aquifers: a numerical solution. Water Resour. Res. 7 (3), 644–657. https://doi.org/10.1029/WR007i003p00644.
Shearman, T.M., Varner, J.M., Hood, S.M., Cansler, C.A., Hiers, J.K., 2019. Modelling post-fire tree mortality: can random forest improve discrimination of imbalanced data? Ecol. Model. 414, 108855. https://doi.org/10.1016/j.ecolmodel.2019.108855.
Shen, G., Yang, X., Jin, Y., Xu, B., Zhou, Q., 2019. Remote sensing and evaluation of the wetland ecological degradation process of the Zoige Plateau Wetland in China. Ecol. Indic. 104, 48–58. https://doi.org/10.1016/j.ecolind.2019.04.063.
Shiroyama, R., Yoshimura, C., 2016. Assessing bluegill (Lepomis macrochirus) habitat suitability using partial dependence function combined with classification approaches. Ecol. Inf. 35, 9–18. https://doi.org/10.1016/j.ecoinf.2016.06.005.
Silliman, B.R., Van De Koppel, J., Bertness, M.D., Stanton, L.E., Mendelssohn, I.A., 2005. Drought, snails, and large-scale die-off of southern US salt marshes. Science. 310 (5755), 1803–1806. https://doi.org/10.1126/science.1118229.
Smart, L.S., Taillie, P.J., Poulter, B., Vukomanovic, J., Singh, K.K., Swenson, J.J., Mitasova, H., Smith, J.W., Meentemeyer, R.K., 2020. Aboveground carbon loss associated with the spread of ghost forests as sea levels rise. Environ. Res. Lett. 15 (10), 104028. https://doi.org/10.1088/1748-9326/aba136.
Souza, C.M., Shimbo, J.Z., Rosa, M.R., Parente, L.L., Alencar, A.A., Rudorff, B.F., Hasenack, H., Matsumoto, M., Ferreira, L.G., Souza-Filho, P.W., de Oliveira, S.W., 2020. Reconstructing three decades of land use and land cover changes in Brazilian biomes with landsat archive and earth engine. Remote Sens. 12 (17), 2735. https://doi.org/10.3390/rs12172735.
Spencer, T., Schuerch, M., Nicholls, R.J., Hinkel, J., Lincke, D., Vafeidis, A.T., Reef, R., McFadden, L., Brown, S., 2016. Global coastal wetland change under sea-level rise and related stresses: The DIVA Wetland Change Model. Glob. Planet. Chang. 139, 15–30. https://doi.org/10.1016/j.gloplacha.2015.12.018.
Stagg, C.L., Osland, M.J., Moon, J.A., Hall, C.T., Feher, L.C., Jones, W.R., Couvillion, B.R., Hartley, S.B., Vervaeke, W.C., 2020. Quantifying hydrologic controls on local-and landscape-scale indicators of coastal wetland loss. Ann. Bot. 125 (2), 365–376. https://doi.org/10.1093/aob/mcz144.
Stehman, S.V., 1997. Selecting and interpreting measures of thematic classification accuracy. Remote Sens. Environ. 62 (1), 77–89. https://doi.org/10.1016/S0034-4257(97)00083-7.
Strobl, C., Boulesteix, A.L., Kneib, T., Augustin, T., Zeileis, A., 2008. Conditional variable importance for random forests. BMC Bioinf. 9 (1), 1. https://doi.org/10.1186/1471-2105-9-307.
Sulova, A., Arsanjani, J.J., 2021. Exploratory analysis of driving force of wildfires in Australia: an application of machine learning within google earth engine. Remote Sens. 13 (1), 1–23. https://doi.org/10.3390/rs13010010.
Sutula, M.A., Stein, E.D., Collins, J.N., Fetscher, A.E., Clark, R., 2006. A practical guide for the development of a wetland assessment method: the California experience. JAWRA J. Am. Water Resour. Assoc. 42 (1), 157–175. https://doi.org/10.1111/j.1752-1688.2006.tb03831.x.
Sweet, W.V., Hamlington, B.D., Kopp, R.E., Weaver, C.P., Barnard, P.L., Bekaert, D., Brooks, W., Craghan, M., Dusek, G., Frederikse, T., Garner, G., Genz, A.S., Krasting, J.P., Larour, E., Marcy, D., Marra, J.J., Obeysekera, J., Osler, M., Pendleton, M., Roman, D., Schmied, L., Veatch, W., White, K.D., Zuzak, C., 2022. Global and Regional Sea level rise scenarios for the United States: updated mean projections and extreme water level probabilities along U.S. Coastlines (NOAA Technical Report NOS 01). National Oceanic and Atmospheric Administration, National Ocean Service, Silver Spring, MD, 111 pp . https://oceanservice.noaa.gov/hazards/sealevelrise/noaa-nostechrpt01-global-regional-SLR-scenarios-US.pdf.
Tahsin, S., Medeiros, S.C., Singh, A., 2016. Resilience of coastal wetlands to extreme hydrologic events in Apalachicola Bay. Geophys. Res. Lett. 43 (14), 7529–7537. https://doi.org/10.1002/2016GL069594.
Tesoriero, A.J., Gronberg, J.A., Juckem, P.F., Miller, M.P., Austin, B.P., 2017. Predicting redox-sensitive contaminant concentrations in groundwater using random forest classification. Water Resour. Res. 53 (8), 7316–7331. https://doi.org/10.1002/2016WR020197.
Tully, K., Gedan, K., Epanchin-Niell, R., Strong, A., Bernhardt, E.S., BenDor, T., Mitchell, M., Kominoski, J., Jordan, T.E., Neubauer, S.C., Weston, N.B., 2019. The invisible flood: the chemistry, ecology, and social implications of coastal saltwater intrusion. BioScience. 69 (5), 368–378. https://doi.org/10.1093/biosci/biz027.
Ury, E.A., Yang, X., Wright, J.P., Bernhardt, E.S., 2021. Rapid deforestation of a coastal landscape driven by sea-level rise and extreme events. Ecol. Appl. 31 (5), e02339. https://doi.org/10.1002/eap.2339.
Van Mensvoort, M.E., Lantin, R.S., Brinkman, R., Van Breemen, N., 1985. Toxicities of wetland soils. Wetland Soils: Characterization, Classification, and Utilization. International Rice Research Institute, Los Baños (Philippines), pp. 123–138.
Vissers, M.J., Frapporti, G., Vriend, S.P., Hoogendoorn, J.H., 1999. The dynamics of groundwater chemistry in unconsolidated aquifers: the Salland section. Phys. Chem. Earth Part B. 24 (6), 529–534. https://doi.org/10.1016/S1464-1909(99)00040-4.
Wasson, K., Woolfolk, A., Fresquez, C., 2013. Ecotones as indicators of changing environmental conditions: rapid migration of salt marsh–upland boundaries. Estuar. Coasts 36 (3), 654–664. https://doi.org/10.1007/s12237-013-9601-8.
Wells, J.T., Kim, S.Y., 1989. Sedimentation in the Albemarle—Pamlico lagoonal system: synthesis and hypotheses. Mar. Geol. 88 (3–4), 263–284. https://doi.org/10.1016/0025-3227(89)90101-1.
Wen, L., Hughes, M., 2020. Coastal wetland mapping using ensemble learning algorithms: a comparative study of bagging, boosting and stacking techniques. Remote Sens. 12 (10), 1683. https://doi.org/10.3390/rs12101683.
Wessels, K.J., Van den Bergh, F., Roy, D.P., Salmon, B.P., Steenkamp, K.C., MacAlister, B., Swanepoel, D., Jewitt, D., 2016. Rapid land cover map updates using change detection and robust random forest classifiers. Remote Sens. 8 (11), 888. https://doi.org/10.3390/rs8110888.
Wetzel, P.R., Kitchens, W.M., 2007. Vegetation change from chronic stress events: detection of the effects of tide gate removal and long-term drought on a tidal marsh. J. Veg. Sci. 18 (3), 431–442. https://doi.org/10.1111/j.1654-1103.2007.tb02555.x.
Williams, K., Pinzon, Z.S., Stumpf, R.P., Raabe, E.A., 1999. Sea-level Rise and Coastal Forests on the Gulf of Mexico. US Geological Survey https://doi.org/10.3133/ofr99441 (122 pp. 1500, 20910).
Williams, K., MacDonald, M., Sternberg, L.D., 2003. Interactions of storm, drought, and sea-level rise on coastal forest: a case study. J. Coast. Res. 1116–1121.
Winter, T.C., 2000. The vulnerability of wetlands to climate change: a hydrologic landscape perspective. JAWRA J. Am. Water Resour. Assoc. 36 (2), 305–311. https://doi.org/10.1111/j.1752-1688.2000.tb04269.x.
Wu, M., Yang, C., Zhang, Y., Lin, N., 2017. Study on driving forces of wetland change in the Western Liaohe River basin based on random forest model. IOP Conference Series: Earth and Environmental Science 2017, Ordos, China, April 14-16, 2017. 012009. https://doi.org/10.1088/1755-1315/64/1/012009.
Yu, X., Yang, J., Graf, T., Koneshloo, M., O'Neal, M.A., Michael, H.A., 2016. Impact of topography on groundwater salinization due to storm surge inundation. Water Resour. Res. 52, 5794–5812. https://doi.org/10.1002/2016WR018814.
Zeng, C., Yang, L., Zhu, A.X., 2017. Construction of membership functions for soil mapping using the partial dependence of soil on environmental covariates calculated by random forest. Soil Sci. Soc. Am. J. 81 (2), 341–353. https://doi.org/10.2136/sssaj2016.06.0195.
Zhang, Y., Li, W., Sun, G., Miao, G., Noormets, A., Emanuel, R., King, J.S., 2018. Understanding coastal wetland hydrology with a new regional-scale, process-based hydrological model. Hydrol. Process. 32 (20), 3158–3173. https://doi.org/10.1002/hyp.13247.
Zhang, Y., Li, W., Sun, G., King, J.S., 2019. Coastal wetland resilience to climate variability: a hydrologic perspective. J. Hydrol. 568, 275–284. https://doi.org/10.1016/j.jhydrol.2018.10.048.
Zhang, X., Chen, G., Cai, L., Jiao, H., Hua, J., Luo, X., Wei, X., 2021a. Impact assessments of typhoon Lekima on forest damages in subtropical China using machine learning methods and landsat 8 OLI imagery. Sustainability. 13 (9), 4893. https://doi.org/10.3390/su13094893.
Zhang, Y., Chen, J., Zhang, J., Zhang, Z., Zhang, M., 2021b. Novel indicator for assessing wetland degradation based on the index of hydrological connectivity and its correlation with the root-soil interface. Ecol. Indic. 133, 108392. https://doi.org/10.1016/j.ecolind.2021.108392.
Zhang, Y., Li, W., Sun, G., King, J., 2022a. Coastal wetland hydrologic resilience to climatic disturbances: concept, quantification, and threshold response. In: Eslamian, S., Eslamian, F. (Eds.), Disaster Risk Reduction for Resilience. Springer, Cham, pp. 417–429 https://doi.org/10.1007/978-3-030-99063-3_18.
Zhang, Y., Svyatsky, D., Rowland, J.C., Moulton, J.D., Cao, Z., Wolfram, P.J., Xu, C., Pasqualini, D., 2022b. Impact of coastal marsh eco-geomorphologic change on saltwater intrusion under future sea level rise. Water Resour. Res. 58 (5). https://doi.org/10.1029/2021WR030333 (e2021WR030333).
Zheng, W., Yang, Z., Wang, X., Wang, H., Yu, X., Wang, L.P., He, B., 2022. Impacts of evaporation and inundation on near-surface salinity at a coastal wetland park. Mar. Pollut. Bull. 185, 114373. https://doi.org/10.1016/j.marpolbul.2022.114373.
Zhu, Z., Woodcock, C.E., 2014. Continuous change detection and classification of land cover using all available Landsat data. Remote Sens. Environ. 144, 152–171. https://doi.org/10.1016/j.rse.2014.01.011.